Signatures of cochlear processing in neuronal coding of auditory information

Nadège Marin, Fernando Lobo Cerna, Jérémie Barral

Signatures of cochlear processing in neuronal coding of auditory information

Nadège Marin[1], Fernando Lobo Cerna[1], and Jérémie Barral[1,2]

[1] Institut de l'Audition, Institut Pasteur, INSERM, Paris, France

[2] CNRS, France

Summary

The vertebrate ear is endowed with remarkable perceptual capabilities. The faintest sounds produce vibrations of magnitudes comparable to those generated by thermal noise and can nonetheless be detected through efficient amplification of small acoustic stimuli. Two mechanisms have been proposed to underlie such sound amplification in the mammalian cochlea: somatic electromotility and active hair-bundle motility. These biomechanical mechanisms may work in concert to tune auditory sensitivity. In addition to amplitude sensitivity, the hearing system shows exceptional frequency discrimination allowing mammals to distinguish complex sounds with great accuracy. For instance, although the wide hearing range of humans encompasses frequencies from 20 Hz to 20 kHz, our frequency resolution extends to one-thirtieth of the interval between successive keys on a piano. In this article, we review the different cochlear mechanisms underlying sound encoding in the auditory system, with a particular focus on the frequency decomposition of sounds. The relation between peak frequency of activation and location along the cochlea – known as tonotopy – arises from multiple gradients in biophysical properties of the sensory epithelium. Tonotopic mapping represents a major organizational principle both in the peripheral hearing system and in higher processing levels and permits the spectral decomposition of complex tones. The ribbon synapses connecting sensory hair cells to auditory afferents and the downstream spiral ganglion neurons are also tuned to process periodic stimuli according to their preferred frequency. Though sensory hair cells and neurons necessarily filter signals beyond a few kHz, many animals can hear well beyond this range. We finally describe how the cochlear structure shapes the neural code for further processing in order to send meaningful information to the brain. Both the phase-locked response of auditory nerve fibers and tonotopy are key to decode sound frequency information and place specific constraints on the downstream neuronal network.

1. Introduction

The role of the hearing system is to convert incoming sound energy into neuronal signals that can be used for downstream perceptual tasks. Broadly speaking, this is achieved using two key processing steps: (1) an impedance matching stage and (2) a mechano-transduction process to relay sound information to the nervous system (Pickles, 2003). The mammalian ear subdivided these tasks across three successive stages: the external ear canal, middle ear, and inner ear (Fig. 1A), which together shape our way of encoding sound information. In this article, we aim to comprehensively review the current and historical understanding of cochlear processing in sound encoding. We further describe how the main principles of processing in the hearing organ define downstream connectivity to shape our sound perception.

The ear achieves remarkable perceptual abilities (Hudspeth, 2014): sharp frequency selectivity, exquisite sensitivity, and operation over a wide dynamic range of sound levels. Although humans are sensitive to a large scale of sound frequencies (20 to 20,000 Hz), we are able to discriminate nearby frequencies that are separated by only 0.2 % (Moore, 1973). The faintest sounds we can hear evoke mechanical vibrations on the eardrum of the order of a picometer (Dalhoff et al., 2007). These properties result from a process that actively amplifies responses to the faintest sounds and sharpens the resonant properties of the ear. The active amplification mechanism compresses sound amplitudes that span over six orders of magnitude into a smaller range of displacements compatible with cellular detection. Although the detailed mechanisms are still under intense investigation, this active process is tightly linked to the transduction of the mechanical input into an electrical signal (Barral and Martin, 2011; Hudspeth, 2014). In the mammalian cochlea, two types of sensory hair cells are activated in response to sound-evoked vibrations of the basilar membrane (Fettiplace and Hackney, 2006). Inner hair cells (IHC) are mainly connected to afferent nerve fibers and send auditory signals to the brain while outer hair cells (OHC) mostly receive inputs from the brain (Spoendlin, 1969). It has been shown that OHCs use metabolic energy to boost sound detection (Hudspeth, 2014): they can actively amplify the sound input by modulating their lengths in response to a change in membrane potential (Brownell et al., 1985), generating a mechano-electrical feedback that can be tuned by the efferent system originating from the brain (Cooper and Guinan, 2006). The bidirectional interaction between the cochlea and the brain is thus central in shaping hearing properties (Guinan, 2006).

Frequency selectivity may arise from various processes, namely the electrical tuning of receptor potentials (Lewis and Hudspeth, 1983), calcium-dependent mechanical feedback (Choe et al., 1998), passive mechanical resonance in accessory structures (Gummer et al., 1996; Nobili et al., 1998; Zwislocki and Kletsky, 1979), or a combination of these (Amro and Neiman, 2014; Weiss, 1982). As these characteristics vary based upon cochlear location, a sound of a given frequency causes resonant vibrations at a given location. The resulting spatial map between cochlear location and best-frequency response, known as tonotopy, is ideally suited to decompose complex sound vibrations according to their frequency content. The cochlea thus behaves as an auditory prism. Still, tonotopy alone might not be sufficient to decode frequency information; temporal information contained in the timing of auditory nerve firing is probably equally important (Schnupp et al., 2011). Indeed, neurons in the auditory nerve fire in phase with the acoustic waveform for frequencies up to 2 kHz (Rose et al., 1967; Taberner and Liberman, 2005), thereby providing direct information about the sound frequency.

The large range of sensitivities, both in terms of intensities and frequencies, places specific limitations on downstream neurons that need to encode very diverse signals. In this review, we describe how the cochlea functions as a frequency analyzer. We then illustrate the different biophysical mechanisms at the level of the cochlea (hair cells, sensory synapses, and

downstream neurons) enabling the transformation of complex sounds into elementary signals. Finally, we detail how this information might be routed to the brain for further processing.

2. Psychoacoustics

The human ear is endowed with great sensitivity. It is able to detect acoustic pressures of p_0 = 20 µPa at a frequency of 1 kHz (Sivian and White, 1933), i.e. a pressure variation five billion times lower than atmospheric pressure. Interferometric measurements revealed that tympanic vibrations as low as 0.5 pm are evoked near the hearing threshold (Dalhoff et al., 2007) and we will detail later how our sensory detectors vibrate with an amplitude of a fraction of a nanometer at this sound level.

The human ear is also sensitive to a wide dynamic range. The use of a logarithmic scale where sound pressure level (SPL) is expressed in decibels (dB) is therefore convenient, such that: $L_{dB\ SPL} = 20 \log (p/p_0)$, where p is the acoustic pressure and p_0 = 20 µPa is a reference sound pressure which is often considered as the threshold of human hearing. From the hearing threshold (0 dB SPL by definition) to the sensation of pain (about 120 dB SPL), the sound amplitude varies by 6 orders of magnitude. This cannot be linearly scaled to the vibrations of the sensory cells, which otherwise would vibrate with an unphysiological amplitude of about 1 mm at the highest sound levels. Similarly, our perception does not vary linearly with sound intensity. The differential threshold, which represents the smallest perceptible difference between the levels of two tones, is proportional to the intensity of the stimulus: $\Delta I_{\min} = kI$, where I is the physical intensity of the stimulus and k a constant equal to 0.12 (Fechner, 1860; Weber, 1851). This corresponds to a variation in intensity of 1 dB SPL and motivates the use of a logarithmic scale to measure sound levels. We thus have 120 perceptual levels to encode 6 orders of magnitude of acoustic pressure. From these observations, it appears that auditory perception is nonlinear and compresses a wide range of intensities into a much lower range of responses.

The perception of pitch is globally related to the periodicity of the acoustic waveform (Oxenham, 2012). Animal species are sensitive to different frequency ranges. For example, while humans hear sounds ranging from 20 Hz to 20 kHz, bats perceive sounds from 2 kHz to 120 kHz. Mammals were thought to be unique in their ability to hear ultrasonic frequencies (i.e. above 20 kHz), but later experiments demonstrated that amphibians produce and perceive sound frequencies up to 35 kHz (Feng et al., 2006). The discrimination of sound frequencies is a determinant factor in various other aspects of hearing, including the sense of pitch and the ability to separate out the different components within a complex sound. Humans have a very accurate ability to discriminate tones whose frequencies differ by only 0.2% around 1 kHz, where our ear is the most sensitive (Moore, 1973). Frequency selectivity fluctuates from 1 to 5% in other species (Fay, 1988), but such measurements are challenging to acquire and often depend on behavioral paradigms.

The perceived intensity of a pure sound is reduced in the presence of a second sound (Fletcher, 1938). This phenomenon, called masking, can seem inconvenient for the purpose of sound detection but is in fact useful when seeking to detect a signal amongst noise. Being nonlinear, masking mainly affects frequency components of low amplitudes and increases the signal-to-noise ratio by suppressing spurious signals. This process could play a significant role in speech intelligibility by increasing contrast (Moore, 2004). Importantly, this masking phenomenon occurs only when frequencies of the masker and signal are sufficiently close. This was established by using a broadband masking noise centered around the test sound. The detection threshold of the test sound increased until the spectral width of the noise reached approximately one fifth of the test frequency (Schooneveldt and Moore, 1989). Experiments such as this bore

the concept of the hearing filter, which corresponds to the width of the critical band of frequencies within which a masking sound affects the detection of a test sound. After numerous psychoacoustic measurements, Zwicker proposed the subdivision of the frequency spectrum into 24 critical bands of different widths (Zwicker, 1961). These bands are narrowest between 1 and 4 kHz, where our frequency selectivity is highest. This notion of critical band has direct applications both for audio file encoding and for cochlear implants where about twenty electrodes are sufficient for speech perception.

These psychoacoustical observations have found various origins in the anatomical, mechanical, and physiological properties of the ear. We will describe these processes in the following sections within the context of the mammalian cochlea. Examples from other animal models will also be given when relevant. Although non-mammalian species face similar constraints with respect to sound detection, they have developed alternative strategies to achieve a similar level of performance.

3. Sound filtering by the outer and middle ear

Sounds are focused by the outer ear, the *pinna* (Fig. 1A), which also functions as a spatial filter and improves sound source localization (Batteau, 1967). Vibrations are then transmitted to the ear canal where a standing wave could settle following a reflection of the acoustic wave on the eardrum. The length $d = 3$ cm of the ear canal imposes a resonant frequency: $f = c/\lambda = c/4d = 2.8\ kHz$. Thus acting as a frequency filter, the ear canal increases pressure oscillations by approximately 10 dB between 2 and 5 kHz (Shaw, 1974), corresponding to our range of best sensitivity.

The acoustic wave, once it reaches the end of the ear canal, sets the tympanic membrane in motion. Its vibrations are transmitted to the oval window of the cochlea via the three ossicles of the middle ear: the hammer (*incus*), the anvil (*malleus*) and the stirrup (*stapes*). The middle ear is the result of a remarkable evolutionary adaptation. Because the mechano-sensitive structures of the inner ear are immersed in fluid, when vertebrates transitioned from aquatic organisms to terrestrial tetrapods, they faced the problem of a difference in impedance between air ($Z_{air} = 430\ Pa \cdot s \cdot m^{-1}$) and water ($Z_{water} = 1.5 \cdot 10^6\ Pa \cdot s \cdot m^{-1}$). A large part of the sound energy is reflected at such an interface, with a transmission coefficient of about 0.1%. As a result, pressure oscillations passing from the gaseous to the liquid medium are attenuated by 30 dB. The middle ear's ability to compensate this attenuation, a phenomenon known as 'impedance matching', relies mainly on the concentration of forces applied to the eardrum onto the much smaller surface of the oval window, where pressure is increased by the ratio of the two areas (Pickles, 2003). Remarkably, the middle ear and its bones appeared in three different forms throughout evolution: in the ancestors of mammals, reptiles, and birds, the latter having only one ossicle. The configuration of the middle ear in mammals as well as the ossified structure of the ossicles favors the transmission of frequencies above 1 kHz (Manley, 1990) and likely allows mammals to perceive frequencies above 10 kHz. In short, the middle ear acts as a lever-arm to efficiently transmit sound vibrations and create a pressure wave in the fluid-filled tube of the cochlea.

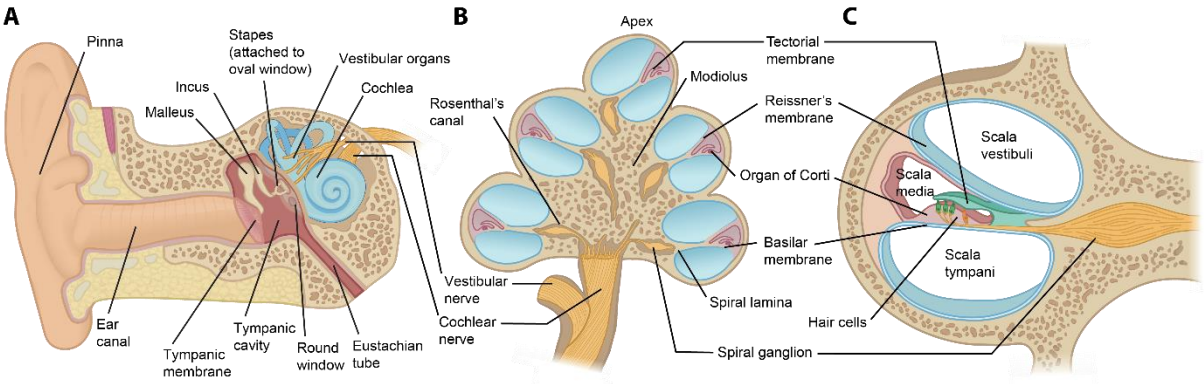

Figure 1: Inner ear anatomy

A. *Anatomy of the human ear including the auditory and the vestibular organs.* ***B.*** *Schematic illustration of a cochlear cross-section showing how the cochlear duct winds around the modiolus containing auditory neurons.* ***C.*** *Expanded view of a cochlear turn cross-section to display the sensory hair cells contacted by spiral ganglion neuron fibers. The scala vestibuli and scala tympani are filled with Na^+-rich perilymph fluid, whereas the scala media, containing the organ of Corti, is filled with K^+-rich endolymph. Note that the scalae vestibuli and tympani connect at the apex. Figure 1 created with BioRender.com and further processed by the authors.*

4. Cochlear mechanics

While the outer and middle ear broadly shape our range of frequency sensitivity, the major psychoacoustical observations discussed above are largely due to the mechanical properties of the inner ear. Sound-induced vibrations propagate along the cochlea, one of the mechanically sensitive organs of the inner ear (Fig. 1A). The cochlea is a duct wound both on itself and around a bony axis known as the *modiolus* (Fig. 1B). In humans, the unrolled cochlea is 35 mm long with a cross section of 2 mm^2. This duct is subdivided into three compartments. In the center, the *scala media* is delimited by the Reissner's membrane and the basilar membrane (Fig. 1C), on which sits the sensory organ of Corti. The upper part of this duct, the vestibular ramp (*scala vestibuli*), is connected to the ossicles of the middle ear by a flexible membrane, the oval window. The lower part, the tympanic ramp (*scala tympani*) presents at its base the round window. Incoming acoustic stimuli cause pressure variations between the *scalae vestibuli* and *tympani* which produce vibrations of the cochlear partition, comprising the basilar membrane, the organ of Corti, the tectorial membrane, the *scala media*, and Reissner's membrane. As a result, the cochlear partition moves in a plane perpendicular to the longitudinal axis of the cochlea. At low sound pressure levels, a pure tone of a given frequency does not displace the full length of the cochlear partition but only sets in motion a small portion of it (Dong et al., 2018; Ren, 2002; Russell and Nilsen, 1997). High-pitched sounds result in vibrations in the basal region of the cochlea, and low-pitched sounds at the apex: this map between position along the cochlea and best-frequency response is called ‘tonotopy’. Although this theory was proposed by Helmholtz during the mid-1800s (Helmholtz, 1863), it was not until a century later that the studies of von Békésy demonstrated a progressive mechanical wave along the cochlea that peaks at a frequency-dependent location (von Békésy, 1956, 1960). This finding offered evidence for the physiological substrate of tonotopy that we will describe in greater details in the following sections. The subsequent auditory processing includes the conversion of mechanical input into electrical signals by specialized sensory cells named inner hair cells (IHCs) sitting on the organ of Corti (Fig. 1C). As described later, a deflection of IHCs’ sensory hair bundles induces the opening of mechano-sensitive channels, leading to the fusion of synaptic vesicles at the afferent connection of the spiral ganglion neurons (SGNs).

4.1. Frequency selectivity

At the beginning of the 19th century, the idea of frequency analysis emerged with the spectral theory formulated by Fourier. Inspired by this framework, Helmholtz stipulated that the cochlea benefits from a set of regularly distributed resonators whose properties systematically vary along its axis (Helmholtz, 1863). The frequency of the incident sound determines which oscillator resonates such that the cochlea behaves like a linear frequency analyzer. A century later, von Békésy combined microscopy and stroboscopic illumination to measure vibrations of the organ of Corti in response to sound stimuli. He observed a progressive wave from the base towards the apex of the cochlea, the amplitude of which presented a maximum at a position that varied according to the sound frequency (von Békésy, 1956, 1960). He established that the characteristic frequency followed an exponential distribution: $f_c = f_b \exp(-x/\lambda)$ where f_b is the preferred frequency at the base of the cochlea and x the position measured from the base. λ is a characteristic length (equal to 7 mm for humans). Assuming that the width of the auditory filter corresponds to a constant length of the basilar membrane, Greenwood confirmed this relationship between characteristic frequency and position along the cochlea (Greenwood, 1961). These findings are consistent with psychoacoustic measurements showing that the sensation of pitch follows a logarithmic distribution (Stevens, 1957) and support the use of the octave in music (doubling of frequency). However, empirical data revealed that a third of the basilar membrane resonates during stimulations, which seems difficult to reconcile with the sharp frequency selectivity evidenced by psychoacoustic experiments.

At the same time, the first electrophysiological measurements were being performed on afferent fibers of the auditory nerve (Galambos and Davis, 1943; Tasaki, 1954) which, although consistent with von Békésy's results, showed rather poor frequency selectivity. The discussion was revived in the early 1970s with the improvement of experimental techniques which made it possible to observe a frequency selectivity at the level of afferent neurons compatible with the critical band of the auditory filter (Evans and Wilson, 1975). These results were interpreted by the existence of a second filter, exclusively of neural origin, which would refine the mechanical filter operated by the basilar membrane. The story could have remained at this stage if the field had not benefited from the Mössbauer technique which involves physically placing a source of gamma radiations on the basilar membrane. When the source is moving, a measurable Doppler shift of the emission allows for the detection of movements of the organ of Corti with sub-nanometric precision (Rhode, 1971; Rhode and Robles, 1974; Sellick et al., 1982). With further technological advances, Sellick observed a good agreement between the sound-pressure level necessary to evoke a vibration of the basilar membrane and an increase in the firing rate of afferent neurons (Sellick et al., 1982). Using laser interferometry, this concordance was subsequently confirmed by simultaneous measurements of the mechanical properties of the basilar membrane and the electrophysiological properties of afferent nerve fibers (Fig. 2A) (Narayan et al., 1998). These experiments thus demonstrated the mechanical origin of neuronal frequency tuning. They also explained that the large width of the mechanical filter observed by von Békésy resulted from the use of cadavers to perform experiments. The frequency selectivity of the cochlea is a physiologically vulnerable phenomenon.

The resonant frequency of a passive mechanical oscillator is proportional to $\sqrt{k/m}$, where k is the stiffness and m is the mass. By demonstrating that the elastic properties vary along the organ of Corti, von Békésy provided a physiological substrate for the theory of resonance which underlies the tonotopy of the cochlea (Table 1). However, stiffness measurements only showed variations of a factor of less than 100. It could not, therefore, explain how humans are sensitive to frequencies ranging from 20 Hz to 20 kHz; the stiffness of the oscillator should, in that case, vary over 6 orders of magnitude if assuming a constant mass (Gummer et al., 1981; Naidu and Mountain, 1998). Later measurements in hemicochlea preparations, more faithful to *in vivo* conditions, showed a better agreement between the characteristic frequency and the quantity

$\sqrt{k/m}$, where stiffness could vary by at least 3 orders of magnitude (Emadi et al., 2004) and a significant variation of mass was due to the morphology of the basilar and tectorial membranes (Richter et al., 2000) (Table 1). The tectorial membrane can indeed contribute to the frequency tuning of the organ of Corti by providing an appropriate scaling of the stiffness (Richter et al., 2007). Because the tectorial membrane is an order of magnitude softer than the basilar membrane, force production by sensory cells may well interact with the tectorial membrane microenvironment (Gueta et al., 2006). This intuition was confirmed *in vivo* using a noninvasive method based on optical coherence tomography which showed that the tectorial membrane was slightly more sharply tuned and that the peak of resonance was more basal than for the basilar membrane (Lee et al., 2015).

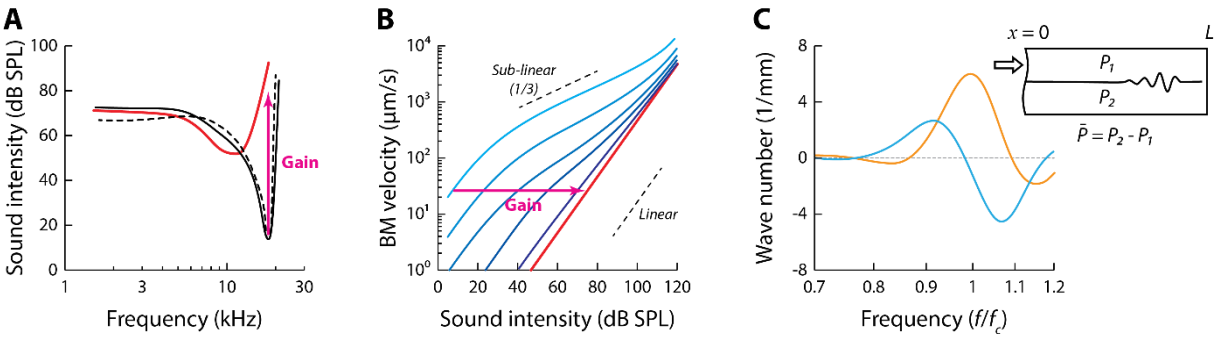

Figure 2: Characterization of cochlear mechanics

A. *Tone level required to achieve threshold movement of the basilar membrane (solid black line: living cochlea; red line: post mortem) or an increase in the rate of discharge of afferent neurons (dotted black line) at a given position along the cochlea (close to its base) as a function of tone frequency. Typical data based on (Narayan et al., 1998; Ruggero et al., 1997).* ***B.*** *Relationship between the velocity of the basilar membrane and the sound level of the stimulus when the tone frequency corresponds to the characteristic place of the basilar membrane (cyan) and for higher frequencies (from cyan to dark blue). The red line corresponds to post-mortem measurements. Linear and sublinear (1/3) scaling are shown for indication. Typical data based on (Ruggero et al., 1997).* ***C.*** *The vibration of the stapes footplate in the oval window induces a pressure difference between the two cochlear compartments (inset). This pressure difference generates a maximal deformation of the basilar membrane at the position corresponding to the characteristic frequency. In the linear regime, the differential pressure $\bar{P} = P_2 - P_1$ propagates along the cochlea with a slow velocity and observes the following wave equation: $(\partial_x^2 + k^2)\bar{P} = 0$, where k is the wave number. Real (orange) and imaginary (blue) part of the wave number as a function of the normalized frequency. Typical data based on (Shera, 2007).*

4.2. Compressive nonlinearity

Measurements from von Békésy were performed on human cadavers with sounds of 100 to 140 dB SPL, greatly exceeding the physiological range of hearing. The reported amplitude of basilar membrane movements was proportional to sound intensity. By extrapolating to a sound near the detection threshold, we would then expect a vibration 500 times smaller than the diameter of a hydrogen atom. Actually, the basilar membrane vibrates with an amplitude of 0.3 nm at the detection threshold (Robles and Ruggero, 2001). At a given position, the measured basilar membrane displacement is sublinear when the stimulation frequency corresponds to the characteristic frequency (Rhode, 1971; Rhode and Robles, 1974). For stimulations ranging from 20 to 80 dB SPL, i.e. three orders of magnitude of sound pressure levels, the response is well described by a power law of exponent 1/3 (Ruggero et al., 1997) (Fig. 2B). The advantage

in terms of dynamic range is obvious with the compression of six orders of magnitude of sound intensity into two orders of magnitude of basilar membrane displacement.

This compressive nonlinearity depends on the sound frequency. Stimulated far from its preferred frequency, the basilar membrane regains a linear behavior (Fig. 2B). Response and stimulus are then proportional, as is the case for a simple spring whose amplitude is proportional to the applied force. It should be noted that the linear behavior of the basilar membrane is asymptotically observed for sound levels of low and large amplitudes.

4.3. Regenerative process and amplification

The organ of Corti is immersed in a viscous fluid which should significantly dampen the vibratory response to sounds. In 1948, Gold challenged the theory of passive resonance (Gold and Pumphrey, 1948). Based on psychoacoustic measurements, he estimated the number of cycles of oscillations that were evoked by very brief pure tones. He could then put a measure on the quality factor (Q) of auditory resonance which is also related to its narrowness in frequency range. Values of Q of 32 to 300 were derived, which seems incompatible with the model of a passive oscillator immersed in a viscous fluid. Gold then suggested the existence of a frequency-selective regenerative process capable of amplification by suppressing part of the viscous losses. Measurements of cochlear mechanics showed that the sound level required to induce a displacement of the basilar membrane of a given amplitude is 50 dB lower when the cochlea is alive (Ruggero and Rich, 1991) ('Gain' in Fig. 2A). Physiological measurements in animal models usually provides quality factor between 1 and 10 with a systematic increase with frequency (Robles and Ruggero, 2001). A notable exception is observed in some bats which devote an extended region of the cochlea, called the acoustic fovea, to echolocation near the frequency of the bat's call. There, an extremely sharp mechanical resonance has been measured on the basilar membrane, with quality factors up to 1,000 (Kossl and Russell, 1995). Humans may also well display a sharper frequency selectivity than mammals studied in the laboratory (Shera et al., 2002).

At a given position of the cochlea, this active mechanism is only effective if the frequency of a sinusoidal stimulation matches the characteristic frequency. Stimulated far from the preferred frequency, the level needed to evoke a given vibration is also increased by 50 dB ('Gain' in Fig. 2B). Not only does amplification depend on the sound frequency, but it also requires energy, since it disappears under hypoxia and postmortem. It is maximal for the weakest stimuli and varies inversely with sound pressure level. It was then proposed that a cochlear amplifier improves hearing sensitivity by delivering energy on a cycle-by-cycle basis (Dallos, 1992; Davis, 1983).

4.4. Cochlear wave

Several studies have shown how different structures of the cochlea vibrate in response to sounds (Olson et al., 2012; Ren et al., 2016; Robles et al., 1986). Due to experimental restrictions, measurements were originally only performed at a single location along the cochlea, but the sound frequency can easily be manipulated. The interferometer technique provides a measure of the speed $V_{BM}(x_0, f)$ of the basilar membrane at a given position x_0 as a function of the sound frequency f. However, the profile of the cochlear wave depends on both. Assuming that the profile of the function $V_{BM}(x, f)$ is minimally modified when x varies, a single variable can be kept: for a given position x, $V_{BM}(x, f) = V_{BM}(f/f_c(x))$, where $f_c(x)$ is the characteristic frequency at position x (de Boer, 1983; Zweig, 1991). As the relationship $f_c(x)$ is known (Greenwood, 1961), it becomes possible to infer $V_{BM}(x, f_0)$ at f_0 fixed (varying x), knowing $V_{BM}(x_0, f)$ at x_0 fixed (varying f).

When BM vibrations are small enough, the pressure difference $\bar{P}$ between the two compartments of the cochlea satisfies a linear wave equation (Lighthill, 1981) (Fig. 2C). It is important to keep in mind that the pressure wave has two components: while the fast wave, traveling at the speed of sound in water (i.e. 1500 m/s), is carried by the average pressure $P_1 + P_2$ which does not induce deformation of the basilar membrane, the pressure difference $P_2 - P_1$ propagates at the same speed as the mechanical deformation of the organ of Corti (i.e. 100 m/s at the base), slows down and stops as it approaches the location corresponding to the characteristic frequency (Ren, 2002; Rhode, 1971). By noting that the basilar membrane's velocity is related to the second derivative of the pressure difference, Shera was able to calculate the local wave number $k(x,f)$ as a function of the velocity of the membrane (Shera, 2007):

$$k^2(x,f) = -\frac{V_{BM}(x,f)}{\int_x^L dx' \int_{x'}^L V_{BM}(x'',f)dx''}$$

The wave number *k* is a complex number. The real part provides information on the propagation of the wave and the imaginary part on its damping: $k(x,f) = \kappa(x,f) + i\gamma(x,f)$. The shape of the real part $\kappa(x,f)$ of the wave vector indicates that the amplitude of vibration increases to reach a maximum at the location of the preferred frequency (Fig. 2C). The imaginary part $\gamma(x,f)$ shows that the wave is first amplified ($\gamma > 0$) up to this point and then attenuated ($\gamma < 0$) (Fig. 2C). This result showed that the organ of Corti actively pumps energy into the cochlear wave upstream of the characteristic position at which resonance takes place. According to this analysis, the inactivation of amplification over a short section of the cochlea basal to the characteristic frequency proved that the cochlear traveling wave accumulates gain as it approaches its peak (Fisher et al., 2012). Pumping energy ahead of the place of resonance is incidentally reproduced in numerous models of cochlear mechanics that show sharp frequency tuning (Ni et al., 2014).

4.5. Tuning at different locations

Although amplification has been reported in all mammals that have been studied experimentally and at every location along the cochlea, several lines of evidence indicate that the active mechanism differs from base to apex. Cooling the whole cochlea resulted in a shift in sensitivity but no change in characteristic frequency of the sensory neurons (Ohlemiller and Siegel, 1994). This effect was more pronounced for high than for low-frequency neurons. Although this method has not been used to measure cochlear mechanics properties, this suggests that active amplification is more sensitive at the base of the cochlea. The assumption of similar profiles at different locations was also challenged by recent experiments using non-invasive tomographic imaging in the intact cochlea. This technique made imaging of several regions of the cochlea possible and demonstrated that the pattern of vibration is fundamentally different from the base to the apex, where amplification gain and frequency selectivity are substantially less pronounced (Dong et al., 2018; Warren et al., 2016).

4.6. Consequences of the active process

4.6.1. Otoacoustic emissions

As previously mentioned, Gold assumed the existence of an active mechanism that injects energy into the system to compensate for the damping due to friction (Gold and Pumphrey, 1948). This mechanism amplifies signals according to their amplitudes and frequencies, but if the gain is too large, the system can become unstable and oscillate spontaneously. In the case of hearing, the ear should then produce sounds. Gold looked for clues of this instability by attempting to directly record any sound emitted from his own ear. Although, his intuition was good, the technical means at his disposal were insufficient. Thirty years later, Kemp succeeded

in demonstrating that energy was emitted from the cochlea by recording an acoustic vibration in the ear canal using an extremely sensitive microphone (Kemp, 1978). The duration of these emitted sounds being longer than the very brief external stimulation which elicited them (a click or a few cycles of oscillation) led to the hypothesis that the ear provides energy. This is also supported by the fact that emitted sounds show a compressive relationship with respect to the stimulus intensity and are of lower intensity in subjects with hearing deficits.

Such emissions can also be present in the absence of any sound (Wilson, 1980; Zurek and Clark, 1981). These spontaneous otoacoustic emissions are generally of low amplitude (less than 20 dB SPL) and attest to the good functioning of the ear. This phenomenon has been widely studied among various animal species. It is present in the four major classes of tetrapods and the frequency of spontaneous emissions coincides with the frequency domain of sensitivity of the species (Bergevin et al., 2008; Manley, 2001; Manley and Köppl, 1998; Probst, 1990). In humans, 70% of people spontaneously emit sounds from their ears. Many arguments support the cochlear origin of otoacoustic emissions (Probst, 1990), which are reduced by agents that block the functioning of hair cells (Anderson and Kemp, 1979) and reversibly disappear under hypoxia (Evans et al., 1981). They are sensitive to the phenomenon of suppressive masking (Zurek and Clark, 1981) as well as to auditory overstimulation (Evans et al., 1981). The round-trip delay of these emissions, measured as the phase-frequency slope (i.e., group delay) is twice as large as the forward delay propagation of the cochlear traveling wave (Kimberley et al., 1993; Ren et al., 2006). This has been deemed evidence of a traveling wave propagating backwards and arguably refutes any possible origin from higher neuronal processes. Finally, otoacoustic emissions have been correlated with spontaneous movements of the basilar membrane (Nuttall et al., 2004) and could in principle interfere with the perception of sounds. The frequency spectrum comprises fairly fine emission bands that may correspond to a mechanism for selecting certain wavelengths, such as in a laser (Shera, 2003). They are characteristic of each individual and could even be used as a biometric indicator (Swabey et al., 2009).

4.6.2. Distortion products and masking

Sharp frequency tuning and amplification result from the nonlinear amplification of small stimuli near the characteristic frequency. Because the ear is nonlinear, it does not transduce sounds with high-fidelity, as evidenced by psychoacoustical studies. First, the perceived loudness of a tone diminishes in the presence of a second tone at a nearby frequency, a phenomenon called masking (Moore, 2004). Second, when listening simultaneously to two pure tones, one can hear not only these frequencies, but also other tones absent from the acoustic stimulus (Goldstein, 1967; Tartini, 1754). Two-tone suppression and distortions have physiological correlates in *in vivo* recordings of basilar membrane vibrations (Robles et al., 1991, 1997; Ruggero et al., 1992). Distortions occur at stimulation amplitudes as small as 30 dB SPL and their relative amplitude is greatest at low sound levels (Robles et al., 1997). These phenomena appear to be intimately related to the nonlinear, frequency-selective active process that enhances sensitivity, sharpens frequency tuning and extends the dynamic range of the cochlea (Robles and Ruggero, 2001). Distorted cochlear vibrations are strong enough to evoke tympanic vibrations (Dalhoff et al., 2007) and be reemitted through the ear canal as distortion-product otoacoustic emissions (Kemp, 1979; Kim et al., 1980; Probst, 1990). Notably, the ears of non-mammalian vertebrates produce similar distortions (Manley et al., 1993; Vassilakis et al., 2004). Like in mammals, this manifestation of nonlinear inner-ear mechanics is associated with active hearing of high sensitivity and sharp frequency selectivity (Manley, 2001). The measurement of distortion products is therefore increasingly used for the detection of early deafness in newborns (Zorowka, 1993).

Distortions and masking have been observed throughout the auditory pathway, starting from the mechanical movements of a single sensory hair cell (Barral and Martin, 2012; Jaramillo et

al., 1993) to the microphonic potential pertaining to the electrical response of an assembly of hair cells (Dallos et al., 1974; Nuttall et al., 2018). The rate of discharge recorded in the afferent fibers of the cochlea reflects both the appearance of distortion products and masking (Kim et al., 1980). In central auditory processing, signs of distortion products have also been observed using magnetoencephalography to detect the presence of beats in the primary auditory cortex (Purcell et al., 2007). It should be noted that masking phenomena can have two distinct origins (Delgutte, 1996). The first is mechanical and directly correlates to the nonlinear amplificatory process that has been described here. The second mechanism is neural: afferent neurons, which discharge in response to the masking sound and enter a refractory state, become temporarily unresponsive during the test sound response.

4.7. Partial summary I: Physiological properties of the cochlea

Auditory information undergoes significant processing at the peripheral level. The main characteristics of hearing – its large dynamic range and its frequency selectivity – stem from the mechanical behavior of the cochlear partition. As such, cochlear vibrations show frequency selectivity and compressive nonlinearity to accommodate a wide range of sound intensities. These properties are characterized by nonlinear masking and distortion products, observable as vibrations of the cochlear partition, which provide a physiological correlate of well described psychoacoustical features. The observation of nonlinear phenomena throughout the hearing pathway suggests that mechanisms involved in the production of distortions and masking happen at an early stage in the auditory process.

The basilar membrane is an elastic lamina whose mechanical properties gradually vary along the cochlear axis and provide the basis for its tonotopy. This mechanical gradient is nevertheless insufficient to explain the frequency selectivity of the hearing filter. To this first passive filter is added a second much more selective filter: an active process within the organ of Corti which, at a given cochlear location, amplifies the vibrations when the sound frequency is less than or equal to the characteristic frequency of the basilar membrane at this position. This amplification, effective at low stimulation amplitudes only, lowers the sensitivity threshold by 50 dB and provides frequency tuning.

Property	Gradient (base to apex)	Putative function	Reference
Organ of Corti biophysics	BM stiffness ↓	Set the resonant frequency	(Emadi et al., 2004; Gummer et al., 1981; Naidu and Mountain, 1998)
	BM cross-section ↑	Set the resonant frequency	(Keiler and Richter, 2001; Richter et al., 2000)
	TM stiffness ↓	Set the resonant frequency	(Gueta et al., 2006; Richter et al., 2007)
	TM dimension ↑	Set the resonant frequency	(Keiler and Richter, 2001; Richter et al., 2000)
HB morphology	Hair bundle length ↑	Set the stiffness of hair cells	(Lim, 1986; Roth and Bruns, 1992; Wright, 1984)
	Stereocilia number ↓	Set the stiffness and determines the MET current	(Lim, 1986; Tilney and Saunders, 1983; Tobin et al., 2019)
HB biophysics	Stiffness ↓	Set the resonant frequency	(Flock and Strelioff, 1984; Tobin et al., 2019)
	Tip-link tension ↓	Set the operating point of HB sensitivity	(Tobin et al., 2019)
Electromotility	OHC length ↑	Stiffness of BM, capacitance, membrane time constant	(Dannhof et al., 1991; Pujol et al., 1992)
	Nonlinear capacitance ↓	Force production	(Santos-Sacchi et al., 1998)

Hair cell intrinsic properties	IHC resting potential ↑	Phasic and sustained response	(Johnson, 2015)
	IHC time constant ↓	Phasic and sustained response	(Johnson, 2015)
	OHC resting potential ↑	Lower time constant	(Johnson et al., 2011)
	OHC time constant ↑	Increased responsiveness to high frequencies	(Johnson et al., 2011)
MET current	IHC resting MET current ↑	Phasic and sustained response	(Johnson, 2015)
	IHC MET conductance →↓	Set the operating point of HB sensitivity	(Beurg et al., 2018; Beurg et al., 2006)
	IHC open probability ↓	Phasic and sustained response	(Johnson, 2015)
	OHC resting MET current ↑	Lower time constant	(Johnson et al., 2011)
	OHC MET conductance ↓	Set the operating point of HB sensitivity	(Beurg et al., 2018; Beurg et al., 2006)
	OHC open probability →	HB sensitivity	(Johnson et al., 2011)
MET kinetics	Activation (turtle cochlea) ↓	Secondary filter	(Ricci et al., 2005)
	Adaptation ↓	Secondary filter	(Kennedy et al., 2003; Ricci et al., 2003; Ricci and Fettiplace, 1997; Ricci et al., 2005)

Table 1: Tonotopic variation of cochlear and hair cell biophysical properties. Abbreviations: BM: basilar membrane, TM: tectorial membrane, HB: hair bundle, MET: mechano-electrical transduction, IHC: inner hair cell, OHC: outer hair cell.

5. Hair cell physiology

The mechanical response of the cochlea is intimately linked to the physical properties of the mechanosensory detectors of the inner ear. Within the organ of Corti are embedded hair cells that transduce sound stimuli into electrical signals (Fig. 3A). We describe in this section how hair cells convert mechanical input into electrical output and shape the mechanical properties of the whole structure.

5.1. Mechanical properties of the hair bundle

The inner ear includes the cochlea but also the vestibular organs devoted to the sense of balance which have very different structures and functions, but, like the cochlea, include hair cells. Hair cells possess a mechano-sensitive organelle called the hair bundle. Their cellular functioning is dependent on deflection of the hair bundle by a mechanical stimulus, rendering them a good model of mechano-electrical transduction (MET), i.e. the conversion of a mechanical stimulus into an electrochemical signal. The hair bundle projects from the apical surface of the cell and is comprised of a few dozen cylindrical rods, the stereocilia. The stereocilia are arranged in rows of increasing length, reminiscent of organ pipes. Each stereocilium is 1-10 µm long, a few hundred nanometers in diameter, and contains a dense bundle of actin filaments (Tilney and Saunders, 1983). When force is applied to the top of the hair bundle, the stereocilia do not bend. More flexible at their base, they pivot at their point of insertion into the cuticular plate (Crawford and Fettiplace, 1985; Flock et al., 1977). Stroboscopic imaging of a hair bundle (Karavitaki and Corey, 2010) as well as interferometric measurements (Kozlov et al., 2011; Kozlov et al., 2007) have shown that movements within the hair bundle are almost perfectly correlated. The hair bundle moves *en masse* so that adjacent stereocilia slide against each other resulting in a stretching of the tip link (Fig. 3B). The tallest row of OHC stereocilia is directly anchored to the tectorial membrane: the movement of the basilar membrane relative to the

tectorial membrane creates a shear which deflects the hair bundle. In contrast, IHCs' hair bundles are not mechanically coupled to this accessory structure and are deflected by fluid motion (Fig. 3A).

Hair cells present notable morphological gradients along the tonotopic axis. From base to apex, hair bundle length increases while stereocilia number decreases (Lim, 1986; Roth and Bruns, 1992; Wright, 1984) (Table 1). These observations were suggested as evidence that hair bundle morphology underlies frequency tuning (Flock and Strelioff, 1984; Turner et al., 1981). These structural gradients are associated with a gradient of physical properties where hair bundle stiffness increases from low to high frequencies (Tobin et al., 2019). The stiffness gradient is not sufficient to explain the range of frequency sensitivity considering a spring-mass system where the resonant frequency of the passive oscillator $\omega_c = \sqrt{k/m}$ is given by the square root of the stiffness *k*. However, the gradient might be sufficient if both characteristic frequency and stiffness follow a linear relation as it is the case for an active oscillator (Hudspeth et al., 2010). Additionally, other gradients may contribute to the regulation of hair bundle stiffness. Because this physical property is also controlled by extracellular Ca^{2+} (Kennedy et al., 2005; Russell et al., 1992), the tight homeostasis of Ca^{2+} concentration along the tonotopic axis is a natural way to set the preferred frequency of the mechanical filters.

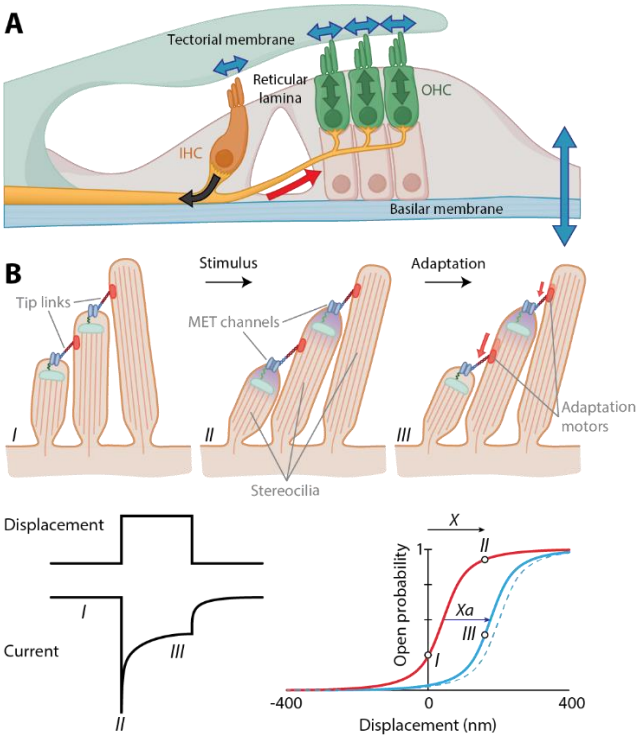

Figure 3: Hair cell mechano-transduction and adaptation

A. *Cartoon transverse section through the sensory organ of Corti of the cochlea, showing how vertical displacement of the basilar membrane (large blue arrow) stimulates the hair cells by bending their stereocilia against the tectorial membrane. Note that IHCs are not connected to the tectorial membrane and are activated by fluid motions generated through this process. Signals from IHCs are relayed to the brain via 10 to 20 afferent fibers of the auditory nerve (black arrow). OHCs have both sensory and motor capabilities through electromotile movements of their basal body (green arrows), which boost cochlear vibrations. They have a sparse afferent innervation (not shown) and are mainly contacted by efferent nerve fibers (red arrow), which regulate somatic electromotility and affect cochlear sensitivity.* ***B.*** *At rest, the non-zero open probability of mechano-transduction channels (red curve) generates a spontaneous current (position I). A positive deflection of the hair bundle (X) increases the*

gating-spring tension materialized by the tip link, leading to an increase of the open probability and an inward current (position II). Adaptation decreases the gating-spring tension which results in a shift (Xa) of the open probability/displacement relationship (blue curve) and a decrease in the transduction current (position III). Note that the shift is smaller than the hair-bundle deflection such that adaptation is incomplete (complete adaptation by a shift X>Xa is shown as the dotted blue curve). Adaptation can be achieved by molecular motors sliding along the actin filaments of the stereocilia. Figure 3A created with BioRender.com and further processed by the authors.

5.2. Mechano-electrical transduction and kinetics

The deflection of the hair bundle induces a receptor current through the cell, called mechano-electrical transduction current, which modifies the transmembrane potential of the cell and creates a receptor potential (Hudspeth, 1985; Hudspeth and Corey, 1977). The mechano-transduction process can be extremely fast, allowing some mammals to hear sounds at frequencies exceeding 100 kHz. This was best demonstrated by recording cochlear microphonics, thought to reflect the mechano-transduction current from OHCs. In the echolocating bat, this measure followed the sound waveform up to 60 kHz (Russell et al., 2003). Hearing is so fast that it cannot be achieved by biochemical reactions, as is the case in other sensory modalities (Corey and Hudspeth, 1979). The open probability of the transduction channels is directly controlled by an increase in tension in an elastic element called the gating spring (Corey and Hudspeth, 1983; Howard and Hudspeth, 1988) (Fig. 3B). The oblique extracellular tip links near the top of the bundle are essential parts of the gating spring as cutting them completely abolishes mechanical transduction (Assad et al., 1991), which can be restored with tip-link regeneration (Zhao et al., 1996).

Direct measurements of transduction kinetics were first made in the bullfrog's sacculus where abrupt deflection of the hair bundle prompts the onset of a transduction current after a delay of only 25 µs at 28°C (Corey and Hudspeth, 1983). In the turtle's auditory organ, channel kinetics shows tonotopic variation: the shortest activation times are observed for cells dedicated to high frequencies (Ricci et al., 2005). This remarkable observation suggests that the transduction activation kinetics helps to define the hair-cell characteristic frequency. In the rat cochlea, activation times of less than 50 µs were measured but remained limited by the rate of stimulation and recording (Kennedy et al., 2003). Using a computational approach to simulate fluctuations of channels' opening and closing, an activation time constant of about 3 µs was recently estimated in mammalian OHCs, compatible with the mouse hearing range (Beurg et al., 2021).

By cutting most of the tip links using a calcium chelator (BAPTA), it was possible to experimentally observe fluctuations in current flow through a single transduction channel, conforming with stochastic transitions between the open and closed states of the MET channel (Crawford et al., 1991; Geleoc et al., 1997; Ricci et al., 2003). As the channel is connected to the gating spring, channels' fluctuations must give rise to intrinsic stochastic forces that can jostle the hair-bundle position, as theoretically suggested (Nadrowski et al., 2004). This intrinsic source of noise, intimately linked to the mechano-sensitivity function of the hair bundle, dominates the hydrodynamic noise owing to the Brownian bombardment of fluid particles and could, in principle, help adjust the characteristic frequency of the hair-bundle response (Barral et al., 2018; Bormuth et al., 2014).

Single channel measurements also corroborate the variation in kinetic properties along the tonotopic axis (Ricci et al., 2003) (Table 1). These results were further confirmed by an increasing number of MET channels in OHCs from the apex to the base (Beurg et al., 2018). Single channel conductance also varies according to cochlear location (Beurg et al., 2006). This

gradient is important because, coupled to a systematic variation in K^+ channel expression on the basal body of hair cells (Mammano and Ashmore, 1996), it effectively decreases the membrane resistance and thus the time constant, letting the membrane potential of OHCs be responsive to fast modulations (Johnson et al., 2011). Similar gradient exists but are less pronounced in IHCs, suggesting a different mode of operation to transduce the sinusoidal sound waveform (Johnson, 2015). In the case of OHCs, cell length systematically increases from base to apex (Dannhof et al., 1991; Pujol et al., 1992). This morphological gradient also contributes to the tonotopy of membrane potential responsiveness, insomuch as capacitance (and hence, membrane time constant) is proportional to the cell surface area (Table 1).

Under physiological conditions, the MET current is mainly carried by potassium (Beurg et al., 2010). Thanks to the highly positive endocochlear potential resulting from an unusually large concentration of K^+ in the endolymph of the *scala media*, the difference in potential on either side of the hair-cell membrane generates a massive driving force for the transport of potassium ions (150 mV in humans). The mechano-sensitive hair bundle exhibits clear directionality: a deflection in the plane of symmetry of the hair bundle directed towards the row of longest stereocilia depolarizes the cell while a stimulus in the opposite direction hyperpolarizes it (Harris et al., 1970; Jones and Milsum, 1970). Stimuli perpendicular to the plane of symmetry have little effect in hair bundles with compact arrangements (Shotwell et al., 1981) but this is less obvious in mammalian cochlear hair cells (Beurg et al., 2016; Marcotti et al., 2014). Pioneer experiments made *in vivo* showed a sigmoidal relationship between hair-cell intracellular currents and sound intensity (Dallos, 1986; Russell and Sellick, 1983). The MET current evoked *in vitro* by a series of step displacements of different amplitudes also resulted in a receptor potential well described by a sigmoid (Hudspeth, 1989; Hudspeth and Corey, 1977) (Fig. 3B). A deflection of a few hundred nanometers is enough to obtain a saturating response (He et al., 2004; Johnson et al., 2011) whereas a hair bundle experiences movements in the nanometer range near the auditory threshold (Chen et al., 2011a). However, the precise range of sensitivity depends on cochlear location, as was shown in a semi-intact hemicochlea preparation where apical OHCs saturated for larger deflections than basal OHCs (He et al., 2004).

The mechano-electrical nonlinearity is associated with the production of distortions that have been observed at the level of the cochlear microphonic, a gross electrical response measured at the round window (Dallos, 1969; Kemp and Brown, 1984). The slope and width of the mechanical nonlinearity probably relies on the concerted deflection of stereocilia, and thus the gating of MET channels, for distortions in the cochlear microphonic response are lost in mutant mice lacking stereocilin (Verpy et al., 2011; Verpy et al., 2008), a component of the top connectors that ensure coherent hair-bundle movements (Kozlov et al., 2011). Mechanical correlates at the level of a single hair-bundle have also demonstrated the role of MET channels' gating (Barral and Martin, 2012; Jaramillo et al., 1993). Hair cells can thus generate prominent electrical distortions that may be relevant for further processing by encoding the sound envelope of high-frequency signals despite the limited bandwidth of downstream neuronal processes (Nuttall et al., 2018).

5.3. Adaptation of the mechano-electrical transduction current

It seems advantageous to set the hair-bundle operating point near an open probability of 0.5 (but see later for the IHC exception). In this case, because a fraction of the channels are open at rest, the cell can be positioned close to the most sensitive range where both depolarizing and hyperpolarizing responses are evoked by positive and negative deflections, respectively (Eatock, 2000). Adaptation can be characterized as a time-dependent shift of the open probability vs displacement relationship along the stimulus axis and has been observed in many species and hair cell types (bullfrog sacculus: (Eatock et al., 1987), turtle: (Crawford et al., 1989), mouse cochlear hair cells: (Kros et al., 1992; Russell et al., 1989), rat cochlea: (Kennedy

et al., 2003)). A positive deflection that opens channels shifts the curve to the right, so channels close; a negative deflection shifts the curve to the left, so they reopen (Fig. 3B). This process allows hair cells to continue responding with high sensitivity when large static stimuli would otherwise saturate the response. Hair cells can adapt to mechanical stimuli on fast and slow timescales (Wu et al., 1999). Fast adaptation occurs when Ca^{2+} enters MET channels and closes them within a few milliseconds or less. It is associated with a hair-bundle movement opposite to the stimulus direction, consistent with the tensioning caused by channel reclosure (Howard and Hudspeth, 1987). Slow adaptation also closes transduction channels, but on a different timescale (10-100 ms). It is associated with a relaxation in the direction of stimulation and requires an active pulling on the gating spring, operated by an assembly of myosin motors climbing on the actin structure (Assad and Corey, 1992; Holt et al., 2002; Howard and Hudspeth, 1987) (Fig. 3B). Typical timescales of both mechanisms seem to vary along the tonotopic axis to match the characteristic frequency (Kennedy et al., 2003; Ricci et al., 2003; Ricci and Fettiplace, 1997) (Table 1). In the turtle and the rat cochleae, the fast component of adaptation is inversely correlated with the preferred frequency to which the cell is sensitive (Ricci et al., 2005). Coupled with the channel activation time that also depends on cochlear position, this creates a broad bandpass filter at the very first stage of mechano-electrical transduction.

5.4. The hair cell as a filtering unit in non-mammalian vertebrates

In non-mammalian vertebrates' inner ear, lacking the cochlear structure and therefore the variations of biophysical properties associated with the tonotopic gradient, two different tuning mechanisms can support the detection of oscillatory stimuli: (1) mechanical oscillations of the hair bundle and (2) electrical oscillations of the membrane potential.

5.4.1. Mechanical oscillations

The most convincing demonstration of the active behavior of hair cells comes from the observation of spontaneous mechanical oscillations of the hair bundle (Martin, 2008). These spontaneous movements have been reported in the cochlea of the turtle (Crawford and Fettiplace, 1985), in the bulb of the semicircular canals of the eel (Rusch and Thurm, 1990) as well as in the saccule of the bullfrog (Denk and Webb, 1992; Howard and Hudspeth, 1987; Martin and Hudspeth, 1999). Although the presence of these movements *in vivo* has not been demonstrated, spontaneous discharge rates may nevertheless show rhythmic activity in the afferent neurons of turtles, lizards, and birds (Manley, 1990).

In the saccule of the bullfrog, hair bundles regularly exhibit spontaneous oscillations when the epithelium is mounted on a chamber containing two compartments that mimic *in vivo* ionic conditions, in particular the low calcium concentration of the endolymph (Martin and Hudspeth, 1999). Hair bundles oscillate at frequencies of 5-50 Hz with a peak-to-peak amplitude of up to 100 nm (Barral et al., 2018). Spontaneous oscillations are ideally suited to detect auditory signals by providing both selective filtering (Martin and Hudspeth, 2001) and amplification of small sinusoidal inputs (Martin and Hudspeth, 1999).

Like adaptation of mechano-transduction, spontaneous oscillations can be modulated by extracellular calcium (Martin et al., 2003). The most astonishing example is the abrupt initiation of spontaneous oscillations when a cell, initially at rest, is subjected to an increase in the calcium concentration (Tinevez et al., 2007). This observation suggests that the hair bundle operates near an oscillatory instability called a Hopf bifurcation (Hudspeth et al., 2010). Calcium controls the dynamic state of the hair bundle (oscillating or quiescent). Under physiological conditions, most hair bundles oscillate spontaneously. Both decrease or increase in calcium concentrations can eliminate these spontaneous oscillations. Calcium homeostasis is thus critical in regulating hair-bundle mechanics by tuning hair-bundle sensitivity and setting the

operating point. A high concentration accelerates the oscillations by a factor of 2 but only decreases the amplitude by 20% (Martin et al., 2003). Interestingly, the modulation of calcium *in vivo* produces the same effects on the otoacoustic emissions of the lizard (Manley et al., 2004). While the lizard's emissions are at much higher frequencies (1-3 kHz), spontaneous activity in these two systems could be produced by a similar mechanism regulated by calcium.

5.4.2. Electrical oscillations

The hair cells of the turtle (Crawford and Fettiplace, 1981) and the chicken (Fuchs et al., 1988) cochleae as well as those from the bullfrog's sacculus (Lewis, 1988) or the gecko auditory papilla (Beurg et al., 2022) all display a phenomenon of electrical resonance. Using patch-clamp, current steps cause a dampened oscillation of the transmembrane potential. By blocking some channels that are located at the base of the hair cells, an interaction between a voltage-dependent calcium current and a large potassium current activated by calcium (BK channels) was demonstrated (Lewis, 1988). Oscillations can arise because of the larger activation time of BK channels. As the limiting step, activation kinetics determines the resonant frequency of the electric oscillator. Along the tonotopic axis of the turtle cochlea, a systematic variation in the activation time ranging from 0.4 to 13 msec has been reported (Art et al., 1995). Interaction with the calcium current then results in a band-pass filter whose characteristic frequency varies as a function of cochlear location (Ricci et al., 2000) and is compatible with the corresponding frequency range of sensitivity (40-600 Hz). In non-mammalian vertebrates, this phenomenon could therefore create a second filter to supplement and refine the frequency selectivity of the hair-bundle amplifier (Fettiplace and Fuchs, 1999).

In some circumstances, the interaction between these two currents can become unstable and generate spontaneous oscillation of the membrane potential, which has been reported in the turtle cochlea (Crawford and Fettiplace, 1980) and in the saccule of the bullfrog (Ashmore, 1983). Similar to mechanical hair-bundle oscillations, electrical oscillations can provide frequency tuning and amplification (Crawford and Fettiplace, 1980) and thus contribute to frequency discrimination.

5.5. Electromotility of mammalian OHCs

Mechanical and electrical oscillations of hair cells have not been reported in mammals. However, mammalian OHCs possess a unique and striking ability: their cell-body length changes with transmembrane potential (Brownell et al., 1985). Patch-clamp application of a depolarizing potential causes the cell soma to contract with a sensitivity of approximately 20 $nm \cdot mV^{-1}$ (Ashmore, 1987). Somatic electromotility could amplify movements of the basilar membrane generated by acoustic stimuli and functions as the required active filter. The mechano-electrical feedback generated by OHC electromotility can be tuned by the efferent system originating from the brain (Cooper and Guinan, 2006). The functional roles of this mediation are still debated, but could include protection from damage caused by loud sounds (Reiter and Liberman, 1995), aided signal-in-noise detection (Winslow and Sachs, 1987), and implication in selective attention (Delano et al., 2007).

Somatic electromotility results from the activity of the prestin protein found in abundant quantities in the basolateral membrane (Zheng et al., 2000). Prestin deletion in mice results in the loss of electromotility *in vitro* and an increase in hearing threshold from 40 to 60 dB SPL *in vivo* (Liberman et al., 2002). Genetic inactivation of the prestin motor without modification of the micromechanical cochlear environment demonstrated its role in amplification (Dallos et al., 2008). The density of prestin, estimated from both capacitance measurements (Corbitt et al., 2012; Santos-Sacchi et al., 1998) and electron microscopy (Mahendrasingam et al., 2010), shows little variation between apical and basal OHCs. However, because OHC length increases from base to apex (Dannhof et al., 1991; Pujol et al., 1992), the force produced by

electromotility may increase along the tonotopic axis and could complement the natural gradient of the basilar membrane to regulate the effective stiffness. These observations make electromotility a prime component of the amplification process within the mammalian cochlea.

However, several points prevent the debate from being closed. First, electromotility is controlled by the transmembrane potential, and not by the receptor current (Santos-Sacchi and Dilger, 1988). The electrical properties of a lipid bilayer in which membrane channels are inserted can be modeled by a capacitance in series with a resistance, hence creating a low-pass filter with a time constant of several milliseconds in most cell types. Even with the fast electrical properties of OHCs, the variable component of the potential would be filtered beyond a frequency neighboring 1 kHz (Santos-Sacchi, 1992), making this mechanism obsolete at high frequencies. Different conclusions have been drawn from tomographic measurements. On the one hand, strongly rectified vibrations showed that OHCs behave as first-order low-pass filters with corner frequencies near 3 kHz, i.e. more than 2.5 octaves below the corresponding characteristic frequencies, and suggested that OHCs rather act as envelope detectors (Vavakou et al., 2019). On the other hand, a detailed examination of the top and bottom displacements of OHCs showed movements in opposite direction at frequencies exceeding 20 kHz, consistent with fast somatic length changes (Dewey et al., 2021). To remedy the problem of low-pass filtering, it was suggested that electromotility does not rely on the transmembrane potential but instead follows the unfiltered extracellular potential (Dallos and Evans, 1995). More recent experiments suggest that the OHC resting membrane potential is sufficiently depolarized (~-50 mV) to activate a voltage-dependent K^+ conductance that shortens the membrane time constant to about 25 µs, which corresponds to a cutoff frequency of 6.4 kHz (Johnson et al., 2011). While this short time constant would extend the frequency response of electromotile movements, the related cutoff frequency remains well below the 10 kHz characteristic frequency of the corresponding hair cell. Finally, how electromotility can function in the upper limit of the auditory range of bats (100 kHz) remains unanswered.

Another issue is that electromotility in itself offers neither non-linearity nor frequency selectivity. A model developed by Nobili and Mammano (Nobili et al., 1998), based on a phase delay between the movements of the tectorial and basilar membranes, displays both. A quarter of cycle of phase delay coupled with the force produced by electromotility contributes a negative frictional force that compensates for viscous drag. When the friction term cancels out, the system is poised at an oscillatory instability which ensures frequency selective amplification (Hudspeth et al., 2010). The linear component of the response vanishes for small sinusoidal stimulations near the preferred frequency of a critical oscillator so that the response of the system becomes essentially nonlinear. But it is still not clear how the properties of the basilar membrane provide the characteristics necessary to its sharp frequency tuning. A theoretical study also proposed a different role for electromotility which could decouple the action of the hair bundle from that of the basilar membrane and reduce the membrane's stiffness towards the apex (Reichenbach and Hudspeth, 2010). This would allow mammals to be sensitive to frequencies well below the limit imposed by the resonant properties of the stiff basilar membrane. Finally, somatic electromotility only exists in mammals, whereas the excellent hearing characteristics described in the introduction, as well as otoacoustic emissions, have been observed in all vertebrates studied so far (Manley and Köppl, 1998).

5.6. Integrating hair-cell force production with cochlear vibrations

Amplification by hair-bundle motility is the only way to boost mechanical vibrations in the non-mammalian inner ear (Manley et al., 2001). In mammals, it is often argued that the force produced by hair-bundle motility is too weak to drive a significant amplification of cochlear vibrations. Yet, in a mouse model lacking the prestin motor, distortion product otoacoustic emissions were still observed for high stimulation amplitudes (Liberman et al., 2004).

Moreover, high level distortion product otoacoustic emissions can also be recorded up to 2 hours postmortem (Rhode, 2007). This suggests that the hair bundle alone, being mechanically coupled to the organ of Corti, can set the cochlear partition in motion without requiring the active amplificatory process. A challenging experiment reproducing the ionic environment of hair cells *in vitro* showed that the receptor potential is not necessary to drive nonlinear amplification, ruling out the involvement of prestin (Chan and Hudspeth, 2005). On the other hand, Ca^{2+} influx through the MET channel was required, supporting the role of hair-bundle motility in the active process.

The necessary ingredients to observe spontaneous oscillations include a mechanical instability characterized by a region of negative stiffness in the force/displacement relationship (Beurg et al., 2008; Kennedy et al., 2005; Russell et al., 1992) and an adaptation mechanism whether based on myosin motors (Tinevez et al., 2007) or on electromotility feedback (O Maoileidigh and Julicher, 2010), both of which are present in mammalian OHCs. However, spontaneous oscillations have never been reported – probably because it is challenging to reproduce the endolymphatic environment of the cochlea. Furthermore, hair-bundle mechanics is often studied after removing the accessory structures anchoring the tips of stereocilia. Recent investigation in cochlea where the tectorial is lifted away from the OHC bundles failed to demonstrate any spontaneous mechanical activity (Quiñones et al., 2022). Indeed, altering the micromechanical environment almost completely eliminates the contribution of inertia which is fundamental in defining hair-bundle response (O Maoileidigh et al., 2012; Salvi et al., 2015; Salvi et al., 2016). The tectorial membrane could provide the necessary load to ensure that hair bundles exert a panoply of motile behaviors and are able to move the organ of Corti (O Maoileidigh and Hudspeth, 2013). Accordingly, the dimensions of both the tectorial and basilar membranes are well regulated along the tonotopic axis (Table 1).

Although an open probability of MET channels near $P_o = 0.5$ places the hair bundle in the most sensitive region for static deflections, this is not the case when driven by sinusoidal stimuli. Because hair cells filter the input according to their membrane time constant, the AC component of IHC becomes neglectable after a few kHz (Russell and Sellick, 1983). For high frequencies, the voltage response is thus dominated by the DC component. In this case, the DC increase in membrane potential is proportional to the DC increase in transduction current. The sigmoidal relationship between transduction current and hair-bundle displacement being approximately symmetrical with respect to $P_o = 0.5$, the transduction current for a hair cell poised there averages to zero, leading to an absence of variation of the filtered membrane potential. However, steady depolarizations can still be evoked. An operating point near $P_o = 0.2$ (i.e. in the region of maximum curvature of the sigmoid) maximizes the integration of the MET current for small stimuli and the resulting sustained depolarization. This might explain the counterintuitive observation that low-frequency IHCs have faster response than cells responding to high frequencies (Johnson, 2015) (Table 1). Being fast-changing, the membrane potential of low frequencies IHCs can follow cochlear vibrations up to a few kHz. Apical IHCs have also an open probability close to 0.5 (Johnson, 2015) (Table 1) which can actually be more efficient to transmit sinusoidal stimuli. At low stimulus amplitude, firing in auditory nerve fibers can be modulated in both direction because there is some spontaneous firing associated with spontaneous release (see 'Signal transmission at the ribbon synapses' below). At high amplitude, synaptic integration is rectified which ensures that positive and negative phases of the receptor potentials will not cancel out. For high frequencies, the hair-cell membrane time constant filters out receptor potentials. Therefore, the combination of low membrane time constant of basal IHCs with an open probability around 0.2 (Johnson, 2015) ensures to efficiently convert sinusoidal sound stimuli into DC receptor potentials (Palmer and Russell, 1986) (see Fig. 4B). With respect to the auditory system as a whole, a higher IHC bandwidth

seems unnecessary as downstream neurons would not be able to follow such fast temporal modulations. The situation for OHCs is different as they need to amplify mechanical vibrations on a cycle-by-cycle basis. Mechanical work provided either by electromotility or hair-bundle motility is maximized near P_o = 0.5. The operating point of OHCs is indeed close to the most sensitive region of MET currents (Cody and Russell, 1987) and their membrane time constants are shorter toward the base, i.e. in areas responding to higher frequencies (Johnson et al., 2011).

The open probability of MET channels at rest is an entry point to mediate certain electrophysiological properties of hair cells, such as their resting membrane potential and, in turn, their effective time constant. Controlling the operation point of hair cells depends on a complex interaction between the tension in the gating spring and Ca^{2+} influx, both of which are tightly regulated along the tonotopic axis with systematic gradients in tip-link tension (Tobin et al., 2019) and single channel conductance (Beurg et al., 2018; Beurg et al., 2006). This segregation of labor between transducers and effectors has been suggested as a general organizing principle, for hair cells in other species also exhibit specific gradients in structural and functional properties along an axis perpendicular to the tonotopic axis (Chiappe et al., 2007).

5.7. Partial summary II: Different tasks for inner and outer hair cells

Despite the severe dissipation of sound vibrations by viscous damping in the cochlea, the mammalian hearing range extends to high frequencies in comparison to other classes of vertebrates. There are two mechanisms proposed for cochlear amplification: somatic electromotility and active hair-bundle motility. In the mammalian cochlea, both processes may act in concert. The active process relies on the function of OHCs, which inject energy back into the system to enhance basilar membrane motions. OHCs are tuned to respond to auditory frequencies, whereas IHCs are specialized in the transmission of auditory signals for further neuronal processing.

6. Sound processing in downstream neuronal networks

6.1. Cochlear innervation

As we detailed in the previous sections, hair cells from the mammalian cochlea have differentiated into two distinct populations: moving away from the center of the spiral, we first encounter a row of inner hair cells, then a group of three rows of outer hair cells (Fig. 3A). These two cell types have distinct connectivity, both from a structural and a functional viewpoint, that leads to the distinction of two apparent subtypes of spiral ganglion neurons (SGNs).

In mature mammals, 95% of SGNs are type I bipolar neurons with myelinated peripheral axons, whose somas are gathered in the *modiolus* (Brown, 1987; Spoendlin, 1972). Each type I afferent fiber is connected to a unique inner hair cell and sends auditory signals toward the brain (Spoendlin, 1969). The 3,000 inner hair cells of the human cochlea are innervated by 30,000 afferent fibers (Nadol, 1988; Ulehlova et al., 1987) such that each IHC receives ~10 nerve terminals (Liberman, 1980), but the precise number varies based upon cochlear location. The mid-frequency range, where perceptual sensitivity is maximal; is more densely innervated than the borders (Ehret, 1979; Spoendlin, 1972) (Table 2). OHCs receive the remaining 5% of SGN afferents, which are thin unipolar and unmyelinated fibers from type II neuron that extend long projections to a dozen of OHCs (Kiang et al., 1982; Liberman et al., 1990).

The mammalian cochlea is modulated by cholinergic feedback from the brainstem via the olivocochlear efferent pathway. About 2,000 efferent neurons, located in the superior olivary

complex, connect hair cells, with contacts evenly distributed between either the basal bodies of OHCs or the afferent synapses of IHCs (Warr and Guinan, 1979). These two types of connectivity outline different modes of operation. The efferent control of OHCs can tune cochlear sensitivity (Wiederhold and Kiang, 1970) by reducing their electromotile contribution to amplification of mechanical vibration of the cochlear partition (Russell and Murugasu, 1997). Alongside, the modulation of afferent terminals provides a way to modulate the excitability, and thus the sensitivity, of type I SGNs (Groff and Liberman, 2003).

6.2. Signal transmission at the ribbon synapses

The receptor potential generated by hair-bundle deflections produces a calcium influx and the fusion of synaptic vesicles located at the hair-cell base where afferent neurons synapse (Fig. 4A). Like photoreceptors, hair cells form ribbon synapses that are ideally suited to ensure sustained rates and produce a graded synaptic response instead of an all-or-none response as found in spiking neurons. In IHCs, each afferent fiber establishes a single synapse with one ribbon (Liberman, 1980; Spoendlin, 1969). Accordingly, the number of synapses is highest in regions of the cochlea that are sensitive to the mid-frequency range (Meyer et al., 2009).

Depolarizations of 20-30 mV induce the release of half the available synaptic pool (Ohn et al., 2016). This estimate makes sense regarding the 50-60 mV depolarization evoked by hair-bundle displacements saturating the MET current (Johnson et al., 2011). Modulations in IHC membrane potential and Ca^{2+} release are nonlinearly related and best fitted by a Boltzmann function with a voltage for half-maximal activation of -28 mV and a 10-90% width of 35 mV (Frank et al., 2009; Ohn et al., 2016). Given the resting membrane potential of IHCs of -70 mV, Ca^{2+} influx is small but partially active in the absence of sound which ensures some spontaneous release and hence spontaneous firing of postsynaptic SGNs. Placing the resting membrane potential close to the voltage for half-maximal activation of Ca^{2+} influx favors sensitivity while dynamic range is guaranteed by a distribution of widths and activation thresholds of individual synapses (Ohn et al., 2016). No tonotopic variation in the activation voltage of Ca^{2+} influx has been observed at this stage and maximizing the dynamic range of responsiveness appears uniformly operated along the cochlea.

The subsequent relationship between Ca^{2+} release and exocytosis strongly depends on the developmental stage. The high Ca^{2+} efficiency of synaptic release by immature IHCs could drive spontaneous neurotransmitter release. In contrast, the low, near-linear Ca^{2+} dependence of exocytosis in mature IHCs may help broaden their dynamic range to encode sound intensity and stimulus envelope with greater precision (Johnson et al., 2005). The Ca^{2+} efficiency of synaptic vesicle release could also depend on cochlear location (Table 2): a linear relationship between changes in membrane capacitance and Ca^{2+} currents was observed in high-frequency regions of the gerbil cochlea, where it may afford increased sensitivity to low-level stimuli as well as more sustained release rates at high intensities (Johnson et al., 2008). In IHCs tuned to lower frequencies, the nonlinearity could instead help to sharpen temporal patterns of synaptic release. This tonotopic variation in the Ca^{2+} dependence of neurotransmitter release is mirrored by a gradient in ribbon synapse morphology, with spherical ribbons being found in apical IHCs and ellipsoid ribbons in basal IHCs. A short distance between presynaptic Ca^{2+} channels and the Ca^{2+} sensors (nanodomain) is essential to trigger exocytosis accurately and may be advantageous for phase-locked responses (Li et al., 2014). Structures of hair cell ribbon synapses vary along the tonotopic axis, with high-frequency cells exploiting microdomain structures, allowing them to better encode a large dynamic range of sound intensities, whereas low-frequency cells operate via nanodomains for precise time encoding (Johnson et al., 2017). As a result, synaptic transmission is probably fast enough to follow mechanical hair-bundle vibrations up to a frequency where the receptor potential is filtered (Li et al., 2014; Wong et al., 2013) (see how the simulated synaptic release of an apical IHC follows the mechanical

stimulation in Fig. 4B). These observations apply generally to auditory coding in vertebrates and are notably valid for the bullfrog's amphibian papilla (Keen and Hudspeth, 2006) and the turtle's amphibian papilla where a gradient of physiological properties also unfolds along the tonotopic axis (Schnee et al., 2005).

In contrast to IHCs, the afferent synapses of OHCs are primarily activated by high sound intensities. Postsynaptic potentials generated by OHCs are of smaller amplitude such that the summation from several OHCs seems necessary to drive firing in the afferent neurons (Weisz et al., 2009). In this light, OHCs have been hypothesized to play a part in signaling the need for shielding the cochlea from loud sounds. Without directly protecting the cochlea, a pain circuit might be ecologically relevant to trigger avoidance of too loud sounds. New studies nevertheless indicate a pathway-specific activation of cochlear nucleus neurons in response to moderate intensities and suggest vesicular glutamate signaling by OHCs to Type II SGNs may participate in acoustic perception at nontraumatic sound levels (Weisz et al., 2021).

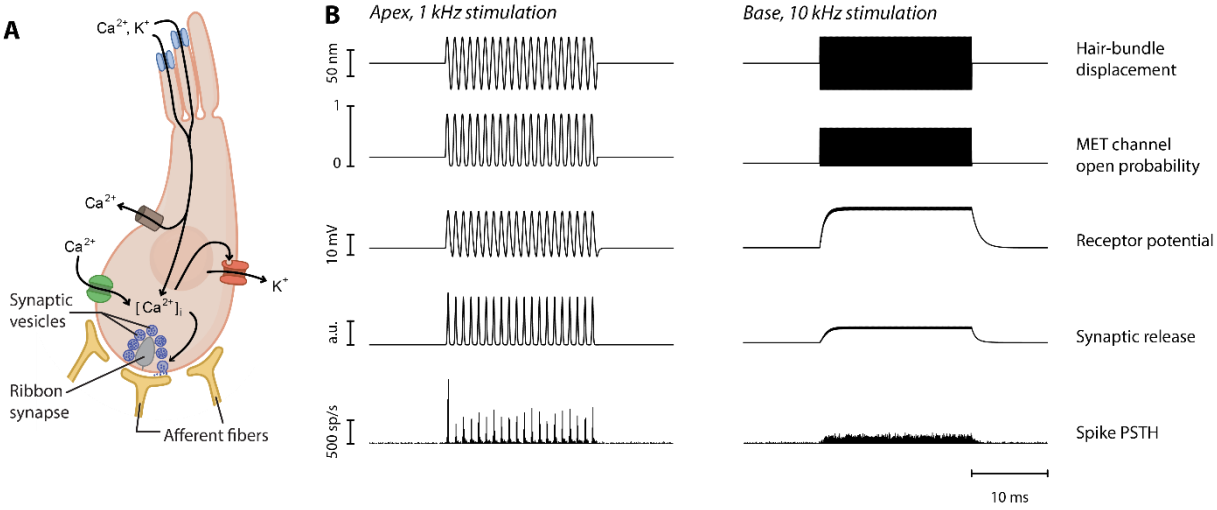

Figure 4: Sound encoding in the auditory nerve
A. *Ionic flow are initiated by the influx of potassium and calcium that ensues from hair-bundle deflection. The induced depolarization opens voltage-dependent calcium channels, raising the concentration of intracellular calcium which in turn leads to the fusion of synaptic vesicles at the ribbon synapse and the generation of a postsynaptic potential in the afferent fibers. Restoration of the membrane potential is made possible by the activation of calcium-dependent potassium channels and the elicited outward K^+ current, while calcium ions are driven out of the hair cell through active transporters.* ***B.*** *Simulation of the cascade of events leading to neuronal firing. Peristimulus time histograms (PSTH) in response to low frequency stimuli are periodic and synchronized with the amplitude modulations of the acoustic waveform at every stage (left panel). Note the sharpening of synaptic release at low frequency. Meanwhile, the membrane time constant of IHCs attenuates the oscillating component of the receptor potential, leading to tonic neurotransmitter release and firing at high frequencies (right panel).*

6.3. Neuronal firing in the spiral ganglion

Synaptic release produces a sufficiently large depolarization in the afferent fiber to evoke an action potential (Glowatzki and Fuchs, 2002; Siegel, 1992). Therefore, spikes can phase lock to the acoustic waveform up to a frequency of about 2 kHz (Rose et al., 1967; Taberner and Liberman, 2005) (see how simulated neuronal firing in Fig. 4B follows the 1 kHz mechanical stimulation). At low levels and frequencies of stimulation, the resulting relationship between the instantaneous acoustic pressure and the discharge rate of auditory nerve fibers is often exponential (Horst et al., 2018). This can result both from the nonlinear mechanics of the

cochlea associated with the amplification of small stimuli and from the link between hair-bundle deflection and receptor potential because the resting open probability of IHCs sets the operating point in a near exponential region. At higher amplitudes, saturation occurs at different levels (transduction current, synaptic release, spike firing) such that the average rate of SGNs displays a sigmoid-like relationship with sound intensity (Taberner and Liberman, 2005).

The intrinsic properties of spiral ganglion neurons exhibit regional variations (Table 2). Using cultures of SGNs, it was reported that neurons connected to hair cells from the base of the cochlea had lower evoked firing rate, shorter spike latency and shorter membrane time constant (Adamson et al., 2002b; Liu and Davis, 2007). These intrinsic electrophysiological properties are mirrored by gradients of voltage and Ca^{2+} gated potassium channels (Adamson et al., 2002a; Adamson et al., 2002b; Chen et al., 2011b). Notably, these systematic gradients are often blurred in a large heterogeneity of intrinsic properties that have been related to different types of K^+ channels (Liu et al., 2014).

Along the tonotopic axis, other features display a bell shape such that SGN spike thresholds are lower at mid-frequency positions, that is, the range of highest frequency selectivity (Liu and Davis, 2007). This region of the cochlea is also innervated by neurons of smaller size (Echteler and Nofsinger, 2000; Liberman and Oliver, 1984), which might be a necessity owing to their intrinsic properties, or a consequence of larger number of SGNs fitting in the confined space of the *modiolus*. Important to neuronal coding strategies is the fact that neurons sensitive to high frequencies often fire a single spike upon prolonged depolarization (Adamson et al., 2002a; Adamson et al., 2002b; Liu and Davis, 2007). This phasic response could make the detection of sound onset and offset more reliable.

Because the hearing dynamic range is outstandingly broad, intensity coding relies on the specialization to different ranges of sound levels (Taberner and Liberman, 2005). Nerve fibers connected to the pillar side of IHCs are spontaneously active and respond to low intensities, whereas neurons synapsing to the modiolar side are silent in the absence of sound and fire at high intensities. This classification is based on *in vivo* physiological recordings, active zone morphology (Kawase and Liberman, 1992; Liberman and Oliver, 1984), as well as intrinsic properties in which more excitable neurons, with lower thresholds and longer membrane time constants *in vitro*, are located on the pillar side of IHCs (Markowitz and Kalluri, 2020). Single-cell profiling investigating the molecular origins of this distribution identified multiple groups of SGNs based on transcriptional identity (Markowitz and Kalluri, 2020; Petitpre et al., 2018; Shrestha et al., 2018; Sun et al., 2018). Correlations between these groups and neuronal physiology have been subsequently established (Sherrill et al., 2019). The diversity in neuronal firing can also result from synaptic mechanisms that take place both at the presynaptic (Frank et al., 2009; Grant et al., 2010; Ozcete and Moser, 2021) and postsynaptic levels (Liberman et al., 2011; Niwa et al., 2021). Finally, it is important to keep in mind that although each SGN fiber is specialized for a given acoustic intensity, they also have the ability to dynamically adapt their dynamic range according to the sound statistics (Wen et al., 2009).

Property	**Gradient (base to apex)**	**Putative function**	**Reference**
IHC synapse	Synapse/cell ↑↓	Increased sensitivity for mid frequencies	(Meyer et al., 2009)
	Activation voltage of Ca^{2+} influx →	Dynamic range	(Ohn et al., 2016)
	Synapse shape (base: ellipsoid, apex: sphere)	Efficiency for high frequencies	(Johnson et al., 2008)
	Synapse distribution (base: microdomain, apex: nanodomain)	Phase locking of low frequencies	(Johnson et al., 2017)

SGN connectivity	Number of afferents ↑↓	Increased sensitivity for mid frequencies	(Ehret, 1979; Meyer et al., 2009; Spoendlin, 1972)
SGN morphology	SGN size ↓↑	Space constraint / intrinsic properties	(Echteler and Nofsinger, 2000; Liberman and Oliver, 1984)
	Axon diameter →	Regulation of conduction delay	(Liberman and Oliver, 1984)
	Fiber length ↑	Regulation of conduction delay	(Liberman and Oliver, 1984)
SGN biophysics	Membrane time constant ↓	Filtering	(Adamson et al., 2002b; Liu and Davis, 2007)
	AP threshold ↓↑	Increased sensitivity for mid frequencies	(Liu and Davis, 2007)
	Max firing rate ↑	Encoding of phasic and sustained component	(Adamson et al., 2002a; Adamson et al., 2002b; Liu and Davis, 2007)

Table 2: Tonotopic variations of synapses and spiral ganglion neurons' biophysical properties. Abbreviations: IHC: inner hair cell, SGN: spiral ganglion neuron, AP: action potential.

6.4. Neuronal coding

The primary function of the brain is to integrate different sensory or cognitive stimuli and to process this information in order to generate an appropriate response, whether motor or cognitive. However, which of the precise characteristics of single neurons and of the network as a whole contribute to setting a proper neural code remains a long-standing question in auditory science and in the field of neuroscience in general. Information may be encoded in several ways.

First, the precise timing of action potentials (*temporal coding*) plays a decisive role by generating temporal sequences. Its relevance to other modalities, such as in motor pathways, has been the focus of much research (Hahnloser et al., 2002; Riehle et al., 1997; Wilent and Contreras, 2005). Timing is obviously important for auditory detection as spikes synchronize with the sound waveform for frequencies up to ~2-4 kHz (Liu et al., 2006; Taberner and Liberman, 2005). Therefore, the sound frequency can be decoded directly using the temporal pattern of neuronal firing.

Second, information can be represented as the average number of action potentials per unit time (*rate coding*). The classical firing scheme includes the modulation of spiking activity in response to the variation of a stimulus attribute: the stretch magnitude of a muscle for proprioception (Adrian and Zotterman, 1926), the motion speed of moving dots for vision (Celebrini and Newsome, 1994), the sound intensity for hearing (Taberner and Liberman, 2005). Coding through firing rate has also been demonstrated in more abstract tasks such as motor planning (Georgopoulos et al., 1982) or perceptual decision (Newsome et al., 1989) functions. In the auditory cortex, some neurons increase their firing rate in response to a pitch of a given frequency (Bendor and Wang, 2005).

Third, information may be represented at the level of the population where each neuron has a distribution of responses to some variation of stimulus attributes and combining the responses of many neurons may determine the precise value of the stimulus. *Population codes* are found in the representation of direction in planned motor movements (Georgopoulos et al., 1986) or saccadic eye movements (Lee et al., 1988). The combination of activities of several neurons is also beneficial from a decoding perspective: by averaging out noise, population activity may represent the input more reliably (Averbeck et al., 2006). Information about sound frequency calls for a population code as a natural consequence of tonotopy. But this needs to be appreciated considering the whole population of the downstream networks. In fact, only a small fraction of neurons in the auditory cortex responds to acoustic stimulations even if the sound falls in their receptive fields (Hromadka et al., 2008). Accordingly, optimizing cortical

population size with relation to the amount of carried information revealed that only a small number of temporally precise neurons is necessary to decode acoustic features (Ince et al., 2013).

It is clear that the nervous system utilizes temporal, rate, and population strategies to encode diverse functions. Rather than being mutually exclusive, there appears to be a continuum between these extreme coding schemes (Kumar et al., 2010). Alternatively, different strategies could be multiplexed and used simultaneously through different coding channels (Panzeri et al., 2010). Encoding sound frequency via timing and intensity via rate is such an example of multiplexing in the auditory system (Sullivan and Konishi, 1984).

6.5. Spatial and temporal coding of frequency

Sound vibrations of different frequencies cause resonances at different locations along the cochlea, owing to the gradients of molecular, cellular and physical properties of the basilar membrane, hair cells and synapses, which have been described here. Tonotopic organization is transmitted to the auditory nerve fibers (Narayan et al., 1998). The frequency map of the cochlea has been reconstructed from labeled neurons recorded in the cochlear nucleus (Muller et al., 2005), which reveals that tonotopy is also propagated to downstream networks. Notably, this map matches the one estimated from critical band measurements with a logarithmic distribution of frequencies (Greenwood, 1961). Tonotopy is then faithfully maintained along the auditory pathway, at least as far as to the thalamus and possibly further to the auditory cortex (Hackett et al., 2011; Kandler et al., 2009). Auditory cortical responses can indeed be predicted with similar performance by decoders whether the model of peripheral auditory processing is spectrogram-based or based on detailed biophysical simulations of the cochlea and auditory nerve (Rahman et al., 2020). This suggests that basic tonotopic mapping is a fundamental coding principle. A recently developed mathematical framework demonstrated how frequency and amplitude can be encoded with a purely spatial map by the location and size of neuronal clusters, respectively (Reyes, 2021). The model accounted for the nonlinear summation of intensity and provided a mechanism for the critical band but lacked the extraction of additional features.

Tonotopy is often viewed as the primary way of encoding frequency information but spatial coding encounters two critical problems. First, the mechanical tuning of the basilar membrane becomes broad when sound intensity is increased (Ruggero et al., 1997). Second, SGNs can phase lock to tones far from their preferred frequency (Rose et al., 1967). These arguments indicate that tonotopy might not be sufficient to decode frequency information and that temporal information is probably equally important (Schnupp et al., 2011). Indeed, neurons in the auditory nerve fire in phase with sound stimulation for frequencies below 2 kHz (Rose et al., 1967; Taberner and Liberman, 2005), thereby providing direct information about the sound frequency (Fig. 4B). In the cat, neurons display a substantial synchronization up to 5 kHz (Johnson, 1980) and in the barn owl, phase locking has been observed up to 10 kHz (Koppl, 1997). Therefore, two cues – spatial and temporal – could be used to decode frequency information but their relative contribution is still highly debated (Verschooten et al., 2019). For high frequencies, sound information seems to be decoded mostly from the tonotopic map since firing is not able to follow the sound waveform. For intermediate and lower frequencies, a dual code might be employed. Even in the auditory cortex, neuronal recordings show enhanced information content when timing is considered as a potential coding scheme (Bizley et al., 2010; Chase and Young, 2007). Notably, temporal information is still available at relatively high frequencies: by summing the activities of several neurons that have a higher probability to fire at a certain phase of the sound stimulus, the volley principle extends the limits fixed by the membrane time constant (Wever and Bray, 1930).

A natural interaction between spatial and temporal coding arises from the delayed propagation of the cochlear wave which ranges from a fraction of millisecond to several milliseconds from base to apex (Ruggero and Temchin, 2007). Conduction delays are also longer at the apex because of substantially longer axon lengths (Liberman and Oliver, 1984) (Table 2). Consequently, high frequency sounds activate downstream neurons after a shorter latency than low frequency sounds (Lin and Guinan, 2000). It is unclear whether these delays are large enough to produce a significant phase shift between fibers originating from a local region of the cochlea (Rattay et al., 2013). However, complex sounds are the summation of several elementary frequencies and neuronal networks able to decode frequency based on the timing of neuronal excitation could conceivably be built, either using recurrent networks or networks based on lags to offset cochlear delays.

6.6. Information flow in the auditory pathway

Information about the external world flows from sensory detectors to the corresponding sensory cortex. Quite uniquely in the auditory system, information crosses many synaptic relays before reaching the auditory cortex. A simple model of such a system is to consider the auditory pathway as a feedforward arrangement of several neurons' pools where propagation occurs without the need of local recurrent activity within a given layer. This architecture seems actually necessary to account for the very small delay of spiking activity in the cortex given the large number of intermediate synapses (Volkov and Galazjuk, 1991). Along the same line, spike latency is shortest for the preferred frequency and for high intensities (Heil and Irvine, 1997; Tan et al., 2008), which suggests that the well-defined tonotopic connection between neuronal structures favors the propagation along a given frequency channel.

The feedforward network model provides a useful and minimal framework for studying information processing in the brain. Several lines of experiments support the model of feedforward networks in biological systems. Propagation of firing rate has been reported in the drosophila olfactory system (Jeanne and Wilson, 2015) and timing is well preserved in the successive layers of the locust auditory system (Vogel and Ronacher, 2007), in the song generation system of the zebra finch bird (Kimpo et al., 2003; Long et al., 2010) or in the visual cortex of the turtle (Hemberger et al., 2019). In the mammalian brain, the model of feedforward network is questioned. Propagation of temporal information is hampered rapidly probably because of significant divergence in synaptic connections, as observed between V1 and V2 areas of the monkey where coordinated events stop after the second stage (Zandvakili and Kohn, 2015). In the thalamocortical system, even if inputs are convergent, they are weak and thus need to be highly synchronous to propagate (Bruno and Sakmann, 2006). Indeed, to propagate temporal information faithfully along the neuronal modules of a feedforward system, two critical parameters must be regulated: the connectivity and the synaptic strength between areas (Diesmann et al., 1999). To maintain tonotopy in the auditory system, the number of divergent connections needs to be controlled accurately so that the signal does not spread. The connectivity parameter is particularly important for the propagation of a pulse of activity: the pulse packet will die out quickly with too many divergent connections if no other mechanism such as recurrent connectivity or NMDA synaptic currents are involved (Barral et al., 2019). Neurons in the cochlear nucleus that receive inputs from SGNs are the most temporally accurate neurons in the brain, with temporal jitter of less than 100 µs. Temporal precision is thus enhanced from the auditory nerve to the cochlear nucleus, and even further in downstream networks (Joris et al., 1994). This can be achieved by anatomical convergence where nearby inputs converge onto one neuron.

Another meaningful result stemming from cochlear mechanics measurements is the width of the cochlear wave. In the gerbil's cochlea, the wavelength of the cochlear wave was estimated at 200 µm for sound intensities close to the hearing threshold (Lee et al., 2015; Ren, 2002). This

means that only a few tens of IHCs oscillate in phase, which has far-reaching implications for neuronal coding at least for low frequencies. Because only a few SGNs will fire synchronously and neurons in the cochlear nucleus only receive a few inputs (Cao and Oertel, 2010), their connections to the downstream neurons need to be sufficiently strong and convergent to enable propagation. Strong connections have indeed been reported along the auditory pathway (Campagnola and Manis, 2014; Romero and Trussell, 2021). Therefore, tonotopic connectivity along the auditory system is not only imperative for maintaining a spatial map of frequency but could also be important for propagating temporally precise input to the cortex. If spikes were asynchronously sent from the cochlea, higher activity would be needed to reach threshold in the next layer. The feedforward architecture with spatially defined channels may help to decrease the amount of spikes needed to propagate the signal and thus the associated metabolic cost. In conclusion, tonotopic mapping represents a major organizational principle both in the peripheral hearing system and in higher processing levels and permits to spectrally decompose complex tones and to preserve this decomposition along the auditory pathway.

7. Future lines of research

The transduction of mechanical displacement of the sensory hair bundle into hair cell depolarization has been well characterized (Beurg et al., 2006; Corey and Hudspeth, 1983). The subsequent transformation of membrane potential into synaptic activity is also well described (Ohn et al., 2016). Yet the hair bundle displacement in response to a sound is unknown. Several experiments have shown how the basilar membrane of the cochlea is vibrating (Ren et al., 2016; Robles et al., 1986). Nevertheless, these measurements were done at a single position along the cochlea. It is now possible to observe several locations using a noninvasive imaging technique which also enables the monitoring of displacements at the hair-cell surface (Lee et al., 2015). However, the hair bundle of inner hair cells is not mechanically coupled to the tectorial membrane. In this regard, it is difficult to know how cochlear vibrations are converted into hair-bundle movements, which ultimately give rise to the receptor potential. Without better knowledge of how the cochlea is activated and sends electrical signals to the brain, neuronal data still remain difficult to interpret. Along the same line, being able to monitor simultaneously several adjacent nerve fibers or auditory fibers from the same IHC may prove highly valuable to understand how phase locking and summation will be processed in downstream networks.

While it is well established that some physical attributes of a sensory stimulus can be decoded using certain features of neuronal activity, it is not clear whether this information is really used by the brain to generate perception (Jacobs et al., 2009; Luna et al., 2005). To understand how sound features are encoded in the brain we would need to (1) vary specific parameters of the sound input, (2) measure how this affects neuronal firing, and (3) determine whether the neural response features that carry sensory information are actually used by the animal to drive behavior. This novel way of looking at neuronal activity is now possible on account of different techniques for perturbing the brain. It has led to the development of a theoretical framework to quantify how much information in the neuronal response is effectively used by the animal to create a sensory percept (Panzeri et al., 2017). Under this framework, significant insight could be gained from measuring whether spatial and temporal information is redundant or synergic at low frequencies.

Declaration of competing interest

The authors declare that their principal affiliations are with not-for-profit organizations and that they have no potential conflict of interest in the publication of this review.

Acknowledgments

We sincerely thank the referees for their careful reading of the manuscript and for their constructive remarks. We also than Keith Doelling and Nathaniel Norberg for providing helpful comments. This work was supported by a Human Frontier Science Program Career Development Award (CDA00009/2017-3), by the CNRS Momentum program and by the Fondation pour l'Audition (FPA IDA01). We acknowledge the support of the Fondation pour l'Audition to the Institut de l'Audition.

References

Adamson, C.L., Reid, M.A., Davis, R.L., 2002a. Opposite actions of brain-derived neurotrophic factor and neurotrophin-3 on firing features and ion channel composition of murine spiral ganglion neurons. J Neurosci 22, 1385-1396.

Adamson, C.L., Reid, M.A., Mo, Z.L., Bowne-English, J., Davis, R.L., 2002b. Firing features and potassium channel content of murine spiral ganglion neurons vary with cochlear location. J Comp Neurol 447, 331-350.

Adrian, E.D., Zotterman, Y., 1926. The impulses produced by sensory nerve-endings: Part II. The response of a Single End-Organ. J Physiol 61, 151-171.

Amro, R.M., Neiman, A.B., 2014. Effect of bidirectional mechanoelectrical coupling on spontaneous oscillations and sensitivity in a model of hair cells. Phys Rev E Stat Nonlin Soft Matter Phys 90, 052704.

Anderson, S.D., Kemp, D.T., 1979. The evoked cochlear mechanical response in laboratory primates. A preliminary report. Arch Otorhinolaryngol 224, 47-54.

Art, J.J., Wu, Y.C., Fettiplace, R., 1995. The calcium-activated potassium channels of turtle hair cells. J Gen Physiol 105, 49-72.

Ashmore, J.F., 1983. Frequency tuning in a frog vestibular organ. Nature 304, 536-538.

Ashmore, J.F., 1987. A fast motile response in guinea-pig outer hair cells: the cellular basis of the cochlear amplifier. J Physiol 388, 323-347.

Assad, J.A., Corey, D.P., 1992. An active motor model for adaptation by vertebrate hair cells. J Neurosci 12, 3291-3309.

Assad, J.A., Shepherd, G.M., Corey, D.P., 1991. Tip-link integrity and mechanical transduction in vertebrate hair cells. Neuron 7, 985-994.

Averbeck, B.B., Latham, P.E., Pouget, A., 2006. Neural correlations, population coding and computation. Nat Rev Neurosci 7, 358-366.

Barral, J., Julicher, F., Martin, P., 2018. Friction from Transduction Channels' Gating Affects Spontaneous Hair-Bundle Oscillations. Biophys J 114, 425-436.

Barral, J., Martin, P., 2011. The physical basis of active mechanosensitivity by the hair-cell bundle. Curr Opin Otolaryngol Head Neck Surg 19, 369-375.

Barral, J., Martin, P., 2012. Phantom tones and suppressive masking by active nonlinear oscillation of the hair-cell bundle. Proc Natl Acad Sci U S A 109, E1344-1351.

Barral, J., Wang, X.J., Reyes, A.D., 2019. Propagation of temporal and rate signals in cultured multilayer networks. Nat Commun 10, 3969.

Batteau, D.W., 1967. The role of the pinna in human localization. Proc R Soc Lond B Biol Sci 168, 158-180.

Bendor, D., Wang, X., 2005. The neuronal representation of pitch in primate auditory cortex. Nature 436, 1161-1165.

Bergevin, C., Freeman, D.M., Saunders, J.C., Shera, C.A., 2008. Otoacoustic emissions in humans, birds, lizards, and frogs: evidence for multiple generation mechanisms. J Comp Physiol A Neuroethol Sens Neural Behav Physiol 194, 665-683.

Beurg, M., Cui, R., Goldring, A.C., Ebrahim, S., Fettiplace, R., Kachar, B., 2018. Variable number of TMC1-dependent mechanotransducer channels underlie tonotopic conductance gradients in the cochlea. Nat Commun 9, 2185.

Beurg, M., Evans, M.G., Hackney, C.M., Fettiplace, R., 2006. A large-conductance calcium-selective mechanotransducer channel in mammalian cochlear hair cells. J Neurosci 26, 10992-11000.

Beurg, M., Gamble, T., Griffing, A.H., Fettiplace, R., 2022. Atypical tuning and amplification mechanisms in gecko auditory hair cells. Proc Natl Acad Sci U S A 119, e2122501119.

Beurg, M., Goldring, A.C., Ricci, A.J., Fettiplace, R., 2016. Development and localization of reverse-polarity mechanotransducer channels in cochlear hair cells. Proc Natl Acad Sci U S A 113, 6767-6772.

Beurg, M., Nam, J.H., Chen, Q., Fettiplace, R., 2010. Calcium balance and mechanotransduction in rat cochlear hair cells. J Neurophysiol 104, 18-34.

Beurg, M., Nam, J.H., Crawford, A., Fettiplace, R., 2008. The actions of calcium on hair bundle mechanics in mammalian cochlear hair cells. Biophys J 94, 2639-2653.

Beurg, M., Nam, J.H., Fettiplace, R., 2021. The speed of the hair cell mechanotransducer channel revealed by fluctuation analysis. J Gen Physiol 153.

Bizley, J.K., Walker, K.M., King, A.J., Schnupp, J.W., 2010. Neural ensemble codes for stimulus periodicity in auditory cortex. J Neurosci 30, 5078-5091.

Bormuth, V., Barral, J., Joanny, J.F., Julicher, F., Martin, P., 2014. Transduction channels' gating can control friction on vibrating hair-cell bundles in the ear. Proc Natl Acad Sci U S A 111, 7185-7190.

Brown, M.C., 1987. Morphology of labeled afferent fibers in the guinea pig cochlea. J Comp Neurol 260, 591-604.

Brownell, W.E., Bader, C.R., Bertrand, D., de Ribaupierre, Y., 1985. Evoked mechanical responses of isolated cochlear outer hair cells. Science 227, 194-196.

Bruno, R.M., Sakmann, B., 2006. Cortex is driven by weak but synchronously active thalamocortical synapses. Science 312, 1622-1627.

Campagnola, L., Manis, P.B., 2014. A map of functional synaptic connectivity in the mouse anteroventral cochlear nucleus. J Neurosci 34, 2214-2230.

Cao, X.J., Oertel, D., 2010. Auditory nerve fibers excite targets through synapses that vary in convergence, strength, and short-term plasticity. J Neurophysiol 104, 2308-2320.

Celebrini, S., Newsome, W.T., 1994. Neuronal and psychophysical sensitivity to motion signals in extrastriate area MST of the macaque monkey. J Neurosci 14, 4109-4124.

Chan, D.K., Hudspeth, A.J., 2005. Ca2+ current-driven nonlinear amplification by the mammalian cochlea in vitro. Nat Neurosci 8, 149-155.

Chase, S.M., Young, E.D., 2007. First-spike latency information in single neurons increases when referenced to population onset. Proc Natl Acad Sci U S A 104, 5175-5180.

Chen, F., Zha, D., Fridberger, A., Zheng, J., Choudhury, N., Jacques, S.L., Wang, R.K., Shi, X., Nuttall, A.L., 2011a. A differentially amplified motion in the ear for near-threshold sound detection. Nat Neurosci 14, 770-774.

Chen, W.C., Xue, H.Z., Hsu, Y.L., Liu, Q., Patel, S., Davis, R.L., 2011b. Complex distribution patterns of voltage-gated calcium channel alpha-subunits in the spiral ganglion. Hear Res 278, 52-68.

Chiappe, M.E., Kozlov, A.S., Hudspeth, A.J., 2007. The structural and functional differentiation of hair cells in a lizard's basilar papilla suggests an operational principle of amniote cochleas. J Neurosci 27, 11978-11985.

Choe, Y., Magnasco, M.O., Hudspeth, A.J., 1998. A model for amplification of hair-bundle motion by cyclical binding of Ca^{2+} to mechanoelectrical-transduction channels. Proc Natl Acad Sci U S A 95, 15321-15326.

Cody, A.R., Russell, I.J., 1987. The response of hair cells in the basal turn of the guinea-pig cochlea to tones. J Physiol 383, 551-569.

Cooper, N.P., Guinan, J.J., Jr., 2006. Efferent-mediated control of basilar membrane motion. J Physiol 576, 49-54.

Corbitt, C., Farinelli, F., Brownell, W.E., Farrell, B., 2012. Tonotopic relationships reveal the charge density varies along the lateral wall of outer hair cells. Biophys J 102, 2715-2724.

Corey, D.P., Hudspeth, A.J., 1979. Response latency of vertebrate hair cells. Biophys J 26, 499-506.

Corey, D.P., Hudspeth, A.J., 1983. Kinetics of the receptor current in bullfrog saccular hair cells. J Neurosci 3, 962-976.

Crawford, A.C., Evans, M.G., Fettiplace, R., 1989. Activation and adaptation of transducer currents in turtle hair cells. J Physiol 419, 405-434.

Crawford, A.C., Evans, M.G., Fettiplace, R., 1991. The actions of calcium on the mechano-electrical transducer current of turtle hair cells. J Physiol 434, 369-398.

Crawford, A.C., Fettiplace, R., 1980. The frequency selectivity of auditory nerve fibres and hair cells in the cochlea of the turtle. J Physiol 306, 79-125.

Crawford, A.C., Fettiplace, R., 1981. An electrical tuning mechanism in turtle cochlear hair cells. J Physiol 312, 377-412.

Crawford, A.C., Fettiplace, R., 1985. The mechanical properties of ciliary bundles of turtle cochlear hair cells. J Physiol 364, 359-379.

Dalhoff, E., Turcanu, D., Zenner, H.P., Gummer, A.W., 2007. Distortion product otoacoustic emissions measured as vibration on the eardrum of human subjects. Proc Natl Acad Sci U S A 104, 1546-1551.

Dallos, P., 1969. Combination tone 2fl-fh in microphonic potentials. J Acoust Soc Am 46, 1437-1444.

Dallos, P., 1986. Neurobiology of cochlear inner and outer hair cells: intracellular recordings. Hear Res 22, 185-198.

Dallos, P., 1992. The active cochlea. J Neurosci 12, 4575-4585.

Dallos, P., Cheatham, M.A., Ferraro, J., 1974. Cochlear mechanics, nonlinearities, and cochlear potentials. J Acoust Soc Am 55, 597-605.

Dallos, P., Evans, B.N., 1995. High-frequency motility of outer hair cells and the cochlear amplifier. Science 267, 2006-2009.

Dallos, P., Wu, X., Cheatham, M.A., Gao, J., Zheng, J., Anderson, C.T., Jia, S., Wang, X., Cheng, W.H., Sengupta, S., He, D.Z., Zuo, J., 2008. Prestin-based outer hair cell motility is necessary for mammalian cochlear amplification. Neuron 58, 333-339.

Dannhof, B.J., Roth, B., Bruns, V., 1991. Length of hair cells as a measure of frequency representation in the mammalian inner ear? Die Naturwissenschaften 78, 570-573.

Davis, H., 1983. An active process in cochlear mechanics. Hear Res 9, 79-90.

de Boer, E., 1983. No sharpening? a challenge for cochlear mechanics. J Acoust Soc Am 73, 567-573.

Delano, P.H., Elgueda, D., Hamame, C.M., Robles, L., 2007. Selective attention to visual stimuli reduces cochlear sensitivity in chinchillas. J Neurosci 27, 4146-4153.

Delgutte, B., 1996. Physiological models for basic auditory percepts. In: Hawkins, H.H., McMullen, T.A., Popper, A.N., Fay, R.R. (Eds.), Auditory computation. Springer, New York, pp. 157-220.

Denk, W., Webb, W.W., 1992. Forward and reverse transduction at the limit of sensitivity studied by correlating electrical and mechanical fluctuations in frog saccular hair cells. Hear Res 60, 89-102.

Dewey, J.B., Altoe, A., Shera, C.A., Applegate, B.E., Oghalai, J.S., 2021. Cochlear outer hair cell electromotility enhances organ of Corti motion on a cycle-by-cycle basis at high frequencies in vivo. Proc Natl Acad Sci U S A 118, e2025206118.

Diesmann, M., Gewaltig, M.O., Aertsen, A., 1999. Stable propagation of synchronous spiking in cortical neural networks. Nature 402, 529-533.

Dong, W., Xia, A., Raphael, P.D., Puria, S., Applegate, B., Oghalai, J.S., 2018. Organ of Corti vibration within the intact gerbil cochlea measured by volumetric optical coherence tomography and vibrometry. J Neurophysiol 120, 2847-2857.

Eatock, R.A., 2000. Adaptation in hair cells. Annu Rev Neurosci 23, 285-314.

Eatock, R.A., Corey, D.P., Hudspeth, A.J., 1987. Adaptation of mechanoelectrical transduction in hair cells of the bullfrog's sacculus. J Neurosci 7, 2821-2836.

Echteler, S.M., Nofsinger, Y.C., 2000. Development of ganglion cell topography in the postnatal cochlea. J Comp Neurol 425, 436-446.

Ehret, G., 1979. Quantitative analysis of nerve fibre densities in the cochlea of the house mouse (Mus musculus). J Comp Neurol 183, 73-88.

Emadi, G., Richter, C.P., Dallos, P., 2004. Stiffness of the gerbil basilar membrane: radial and longitudinal variations. J Neurophysiol 91, 474-488.

Evans, E.F., Wilson, J.P., 1975. Cochlear tuning properties: concurrent basilar membrane and single nerve fiber measurements. Science 190, 1218-1221.

Evans, E.F., Wilson, J.P., Borerwe, T.A., 1981. Animal models of tinnitus. Ciba Found Symp 85, 108-138.

Fay, R.R., 1988. Comparative psychoacoustics. Hear Res 34, 295-305.

Fechner, G.T., 1860. Elemente der Psychophysik, Leipzig.

Feng, A.S., Narins, P.M., Xu, C.H., Lin, W.Y., Yu, Z.L., Qiu, Q., Xu, Z.M., Shen, J.X., 2006. Ultrasonic communication in frogs. Nature 440, 333-336.

Fettiplace, R., Fuchs, P.A., 1999. Mechanisms of hair cell tuning. Annu Rev Physiol 61, 809-834.

Fettiplace, R., Hackney, C.M., 2006. The sensory and motor roles of auditory hair cells. Nat Rev Neurosci 7, 19-29.

Fisher, J.A., Nin, F., Reichenbach, T., Uthaiah, R.C., Hudspeth, A.J., 2012. The spatial pattern of cochlear amplification. Neuron 76, 989-997.

Fletcher, H., 1938. The mechanism of hearing as revealed through experiment of the masking effect of thermal noise. Proceedings of the National Academy of Sciences of the United States of America 24, 265-274.

Flock, A., Flock, B., Murray, E., 1977. Studies on the sensory hairs of receptor cells in the inner ear. Acta Otolaryngol 83, 85-91.

Flock, A., Strelioff, D., 1984. Graded and nonlinear mechanical properties of sensory hairs in the mammalian hearing organ. Nature 310, 597-599.

Frank, T., Khimich, D., Neef, A., Moser, T., 2009. Mechanisms contributing to synaptic Ca2+ signals and their heterogeneity in hair cells. Proc Natl Acad Sci U S A 106, 4483-4488.

Fuchs, P.A., Nagai, T., Evans, M.G., 1988. Electrical tuning in hair cells isolated from the chick cochlea. J Neurosci 8, 2460-2467.

Galambos, R., Davis, J., 1943. The response of single auditory nerve fibers to acoustic stimulation. J Neurophysiol 6, 39-57.

Geleoc, G.S., Lennan, G.W., Richardson, G.P., Kros, C.J., 1997. A quantitative comparison of mechanoelectrical transduction in vestibular and auditory hair cells of neonatal mice. Proc Biol Sci 264, 611-621.

Georgopoulos, A.P., Kalaska, J.F., Caminiti, R., Massey, J.T., 1982. On the relations between the direction of two-dimensional arm movements and cell discharge in primate motor cortex. J Neurosci 2, 1527-1537.

Georgopoulos, A.P., Schwartz, A.B., Kettner, R.E., 1986. Neuronal population coding of movement direction. Science 233, 1416-1419.

Glowatzki, E., Fuchs, P.A., 2002. Transmitter release at the hair cell ribbon synapse. Nat Neurosci 5, 147-154.

Gold, T., Pumphrey, R.J., 1948. Hearing. I. The cochlea as a frequency analyser. Proc. R. Soc. London B 135, 462-491.

Goldstein, J.L., 1967. Auditory nonlinearity. J Acoust Soc Am 41, 676-689.

Grant, L., Yi, E., Glowatzki, E., 2010. Two modes of release shape the postsynaptic response at the inner hair cell ribbon synapse. J Neurosci 30, 4210-4220.

Greenwood, D., 1961. Critical Bandwidth and Frequency Coordinates of Basilar Membrane. Journal of the Acoustical Society of America 33, 1344-&.

Groff, J.A., Liberman, M.C., 2003. Modulation of cochlear afferent response by the lateral olivocochlear system: activation via electrical stimulation of the inferior colliculus. J Neurophysiol 90, 3178-3200.

Gueta, R., Barlam, D., Shneck, R.Z., Rousso, I., 2006. Measurement of the mechanical properties of isolated tectorial membrane using atomic force microscopy. Proc Natl Acad Sci U S A 103, 14790-14795.

Guinan, J.J., Jr., 2006. Olivocochlear efferents: anatomy, physiology, function, and the measurement of efferent effects in humans. Ear Hear 27, 589-607.

Gummer, A.W., Hemmert, W., Zenner, H.P., 1996. Resonant tectorial membrane motion in the inner ear: its crucial role in frequency tuning. Proc Natl Acad Sci U S A 93, 8727-8732.

Gummer, A.W., Johnstone, B.M., Armstrong, N.J., 1981. Direct Measurement of Basilar-Membrane Stiffness in the Guinea-Pig. Journal of the Acoustical Society of America 70, 1298-1309.

Hackett, T.A., Barkat, T.R., O'Brien, B.M., Hensch, T.K., Polley, D.B., 2011. Linking topography to tonotopy in the mouse auditory thalamocortical circuit. J Neurosci 31, 2983-2995.

Hahnloser, R.H., Kozhevnikov, A.A., Fee, M.S., 2002. An ultra-sparse code underlies the generation of neural sequences in a songbird. Nature 419, 65-70.

Harris, G.G., Frishkopf, L.S., Flock, A., 1970. Receptor potentials from hair cells of the lateral line. Science 167, 76-79.

He, D.Z., Jia, S., Dallos, P., 2004. Mechanoelectrical transduction of adult outer hair cells studied in a gerbil hemicochlea. Nature 429, 766-770.

Heil, P., Irvine, D.R., 1997. First-spike timing of auditory-nerve fibers and comparison with auditory cortex. J Neurophysiol 78, 2438-2454.

Helmholtz, 1863. Die Lehre von den Tonempfindungen als physiologische Grundlage für die Theorie der Musik. Braunschweig.

Hemberger, M., Shein-Idelson, M., Pammer, L., Laurent, G., 2019. Reliable Sequential Activation of Neural Assemblies by Single Pyramidal Cells in a Three-Layered Cortex. Neuron 104, 353-369 e355.

Holt, J.R., Gillespie, S.K., Provance, D.W., Shah, K., Shokat, K.M., Corey, D.P., Mercer, J.A., Gillespie, P.G., 2002. A chemical-genetic strategy implicates myosin-1c in adaptation by hair cells. Cell 108, 371-381.

Horst, J.W., McGee, J., Walsh, E.J., 2018. Input-output curves of low and high spontaneous rate auditory nerve fibers are exponential near threshold. Hear Res 367, 195-206.

Howard, J., Hudspeth, A.J., 1987. Mechanical relaxation of the hair bundle mediates adaptation in mechanoelectrical transduction by the bullfrog's saccular hair cell. Proc Natl Acad Sci U S A 84, 3064-3068.

Howard, J., Hudspeth, A.J., 1988. Compliance of the hair bundle associated with gating of mechanoelectrical transduction channels in the bullfrog's saccular hair cell. Neuron 1, 189-199.

Hromadka, T., Deweese, M.R., Zador, A.M., 2008. Sparse representation of sounds in the unanesthetized auditory cortex. PLoS Biol 6, e16.

Hudspeth, A.J., 1985. The cellular basis of hearing: the biophysics of hair cells. Science 230, 745-752.

Hudspeth, A.J., 1989. How the ear's works work. Nature 341, 397-404.

Hudspeth, A.J., 2014. Integrating the active process of hair cells with cochlear function. Nat Rev Neurosci 15, 600-614.

Hudspeth, A.J., Corey, D.P., 1977. Sensitivity, polarity, and conductance change in the response of vertebrate hair cells to controlled mechanical stimuli. Proc Natl Acad Sci U S A 74, 2407-2411.

Hudspeth, A.J., Julicher, F., Martin, P., 2010. A critique of the critical cochlea: Hopf--a bifurcation--is better than none. J Neurophysiol 104, 1219-1229.

Ince, R.A., Panzeri, S., Kayser, C., 2013. Neural codes formed by small and temporally precise populations in auditory cortex. J Neurosci 33, 18277-18287.

Jacobs, A.L., Fridman, G., Douglas, R.M., Alam, N.M., Latham, P.E., Prusky, G.T., Nirenberg, S., 2009. Ruling out and ruling in neural codes. Proc Natl Acad Sci U S A 106, 5936-5941.

Jaramillo, F., Markin, V.S., Hudspeth, A.J., 1993. Auditory illusions and the single hair cell. Nature 364, 527-529.

Jeanne, J.M., Wilson, R.I., 2015. Convergence, Divergence, and Reconvergence in a Feedforward Network Improves Neural Speed and Accuracy. Neuron 88, 1014-1026.

Johnson, D.H., 1980. The relationship between spike rate and synchrony in responses of auditory-nerve fibers to single tones. J Acoust Soc Am 68, 1115-1122.

Johnson, S.L., 2015. Membrane properties specialize mammalian inner hair cells for frequency or intensity encoding. Elife 4, e08177.

Johnson, S.L., Beurg, M., Marcotti, W., Fettiplace, R., 2011. Prestin-driven cochlear amplification is not limited by the outer hair cell membrane time constant. Neuron 70, 1143-1154.

Johnson, S.L., Forge, A., Knipper, M., Munkner, S., Marcotti, W., 2008. Tonotopic variation in the calcium dependence of neurotransmitter release and vesicle pool replenishment at mammalian auditory ribbon synapses. J Neurosci 28, 7670-7678.

Johnson, S.L., Marcotti, W., Kros, C.J., 2005. Increase in efficiency and reduction in Ca2+ dependence of exocytosis during development of mouse inner hair cells. J Physiol 563, 177-191.

Johnson, S.L., Olt, J., Cho, S., von Gersdorff, H., Marcotti, W., 2017. The Coupling between Ca(2+) Channels and the Exocytotic Ca(2+) Sensor at Hair Cell Ribbon Synapses Varies Tonotopically along the Mature Cochlea. J Neurosci 37, 2471-2484.

Jones, G.M., Milsum, J.H., 1970. Characteristics of neural transmission from the semicircular canal to the vestibular nuclei of cats. J Physiol 209, 295-316.

Joris, P.X., Carney, L.H., Smith, P.H., Yin, T.C., 1994. Enhancement of neural synchronization in the anteroventral cochlear nucleus. I. Responses to tones at the characteristic frequency. J Neurophysiol 71, 1022-1036.

Kandler, K., Clause, A., Noh, J., 2009. Tonotopic reorganization of developing auditory brainstem circuits. Nat Neurosci 12, 711-717.

Karavitaki, K.D., Corey, D.P., 2010. Sliding adhesion confers coherent motion to hair cell stereocilia and parallel gating to transduction channels. J Neurosci 30, 9051-9063.

Kawase, T., Liberman, M.C., 1992. Spatial organization of the auditory nerve according to spontaneous discharge rate. J Comp Neurol 319, 312-318.

Keen, E.C., Hudspeth, A.J., 2006. Transfer characteristics of the hair cell's afferent synapse. Proc Natl Acad Sci U S A 103, 5537-5542.

Keiler, S., Richter, C.P., 2001. Cochlear dimensions obtained in hemicochleae of four different strains of mice: CBA/CaJ, 129/CD1, 129/SvEv and C57BL/6J. Hearing Research 162, 91-104.

Kemp, D.T., 1978. Stimulated acoustic emissions from within the human auditory system. J Acoust Soc Am 64, 1386-1391.

Kemp, D.T., 1979. Evidence of mechanical nonlinearity and frequency selective wave amplification in the cochlea. Arch Otorhinolaryngol 224, 37-45.

Kemp, D.T., Brown, A.M., 1984. Ear canal acoustic and round window electrical correlates of 2f1-f2 distortion generated in the cochlea. Hear Res 13, 39-46.

Kennedy, H.J., Crawford, A.C., Fettiplace, R., 2005. Force generation by mammalian hair bundles supports a role in cochlear amplification. Nature 433, 880-883.

Kennedy, H.J., Evans, M.G., Crawford, A.C., Fettiplace, R., 2003. Fast adaptation of mechanoelectrical transducer channels in mammalian cochlear hair cells. Nat Neurosci 6, 832-836.

Kiang, N.Y., Rho, J.M., Northrop, C.C., Liberman, M.C., Ryugo, D.K., 1982. Hair-cell innervation by spiral ganglion cells in adult cats. Science 217, 175-177.

Kim, D.O., Molnar, C.E., Matthews, J.W., 1980. Cochlear mechanics: nonlinear behavior in two-tone responses as reflected in cochlear-nerve-fiber responses and in ear-canal sound pressure. J Acoust Soc Am 67, 1704-1721.

Kimberley, B.P., Brown, D.K., Eggermont, J.J., 1993. Measuring human cochlear traveling wave delay using distortion product emission phase responses. J Acoust Soc Am 94, 1343-1350.

Kimpo, R.R., Theunissen, F.E., Doupe, A.J., 2003. Propagation of correlated activity through multiple stages of a neural circuit. J Neurosci 23, 5750-5761.

Koppl, C., 1997. Phase locking to high frequencies in the auditory nerve and cochlear nucleus magnocellularis of the barn owl, Tyto alba. J Neurosci 17, 3312-3321.

Kossl, M., Russell, I.J., 1995. Basilar membrane resonance in the cochlea of the mustached bat. Proc Natl Acad Sci U S A 92, 276-279.

Kozlov, A.S., Baumgart, J., Risler, T., Versteegh, C.P., Hudspeth, A.J., 2011. Forces between clustered stereocilia minimize friction in the ear on a subnanometre scale. Nature 474, 376-379.

Kozlov, A.S., Risler, T., Hudspeth, A.J., 2007. Coherent motion of stereocilia assures the concerted gating of hair-cell transduction channels. Nat Neurosci 10, 87-92.

Kros, C.J., Rusch, A., Richardson, G.P., 1992. Mechano-electrical transducer currents in hair cells of the cultured neonatal mouse cochlea. Proc Biol Sci 249, 185-193.

Kumar, A., Rotter, S., Aertsen, A., 2010. Spiking activity propagation in neuronal networks: reconciling different perspectives on neural coding. Nat Rev Neurosci 11, 615-627.

Lee, C., Rohrer, W.H., Sparks, D.L., 1988. Population coding of saccadic eye movements by neurons in the superior colliculus. Nature 332, 357-360.

Lee, H.Y., Raphael, P.D., Park, J., Ellerbee, A.K., Applegate, B.E., Oghalai, J.S., 2015. Noninvasive in vivo imaging reveals differences between tectorial membrane and basilar membrane traveling waves in the mouse cochlea. Proc Natl Acad Sci U S A 112, 3128-3133.

Lewis, E.R., 1988. Tuning in the bullfrog ear. Biophys J 53, 441-447.

Lewis, R.S., Hudspeth, A.J., 1983. Voltage- and ion-dependent conductances in solitary vertebrate hair cells. Nature 304, 538-541.

Li, G.L., Cho, S., von Gersdorff, H., 2014. Phase-locking precision is enhanced by multiquantal release at an auditory hair cell ribbon synapse. Neuron 83, 1404-1417.

Liberman, L.D., Wang, H., Liberman, M.C., 2011. Opposing gradients of ribbon size and AMPA receptor expression underlie sensitivity differences among cochlear-nerve/hair-cell synapses. J Neurosci 31, 801-808.

Liberman, M.C., 1980. Efferent synapses in the inner hair cell area of the cat cochlea: an electron microscopic study of serial sections. Hear Res 3, 189-204.

Liberman, M.C., Dodds, L.W., Pierce, S., 1990. Afferent and efferent innervation of the cat cochlea: quantitative analysis with light and electron microscopy. J Comp Neurol 301, 443-460.

Liberman, M.C., Gao, J., He, D.Z., Wu, X., Jia, S., Zuo, J., 2002. Prestin is required for electromotility of the outer hair cell and for the cochlear amplifier. Nature 419, 300-304.

Liberman, M.C., Oliver, M.E., 1984. Morphometry of intracellularly labeled neurons of the auditory nerve: correlations with functional properties. J Comp Neurol 223, 163-176.

Liberman, M.C., Zuo, J., Guinan, J.J., Jr., 2004. Otoacoustic emissions without somatic motility: can stereocilia mechanics drive the mammalian cochlea? J Acoust Soc Am 116, 1649-1655.

Lighthill, J., 1981. Energy-Flow in the Cochlea. Journal of Fluid Mechanics 106, 149-213.

Lim, D.J., 1986. Functional structure of the organ of Corti: a review. Hear Res 22, 117-146.

Lin, T., Guinan, J.J., Jr., 2000. Auditory-nerve-fiber responses to high-level clicks: interference patterns indicate that excitation is due to the combination of multiple drives. J Acoust Soc Am 107, 2615-2630.

Liu, L.F., Palmer, A.R., Wallace, M.N., 2006. Phase-locked responses to pure tones in the inferior colliculus. J Neurophysiol 95, 1926-1935.

Liu, Q., Davis, R.L., 2007. Regional specification of threshold sensitivity and response time in CBA/CaJ mouse spiral ganglion neurons. J Neurophysiol 98, 2215-2222.

Liu, Q., Lee, E., Davis, R.L., 2014. Heterogeneous intrinsic excitability of murine spiral ganglion neurons is determined by Kv1 and HCN channels. Neuroscience 257, 96-110.

Long, M.A., Jin, D.Z., Fee, M.S., 2010. Support for a synaptic chain model of neuronal sequence generation. Nature 468, 394-399.

Luna, R., Hernandez, A., Brody, C.D., Romo, R., 2005. Neural codes for perceptual discrimination in primary somatosensory cortex. Nat Neurosci 8, 1210-1219.

Mahendrasingam, S., Beurg, M., Fettiplace, R., Hackney, C.M., 2010. The ultrastructural distribution of prestin in outer hair cells: a post-embedding immunogold investigation of low-frequency and high-frequency regions of the rat cochlea. Eur J Neurosci 31, 1595-1605.

Mammano, F., Ashmore, J.F., 1996. Differential expression of outer hair cell potassium currents in the isolated cochlea of the guinea-pig. J Physiol 496 (Pt 3), 639-646.

Manley, G.A., 1990. Peripheral hearing mechanisms in reptiles and birds. Springer-Verlag, Berlin.

Manley, G.A., 2001. Evidence for an active process and a cochlear amplifier in nonmammals. J Neurophysiol 86, 541-549.

Manley, G.A., Kirk, D.L., Koppl, C., Yates, G.K., 2001. In vivo evidence for a cochlear amplifier in the hair-cell bundle of lizards. Proc Natl Acad Sci U S A 98, 2826-2831.

Manley, G.A., Köppl, C., 1998. Phylogenic development of the cochlea and its innervation. Curr. Opin. Neurobiol. 8, 468-474.

Manley, G.A., Köppl, C., Johnstone, B.M., 1993. Distortion-product otoacoustic emissions in the bobtail lizard. I: General characteristics. The Journal of the Acoustical Society of America 93, 2820-2833.

Manley, G.A., Sienknecht, U., Koppl, C., 2004. Calcium modulates the frequency and amplitude of spontaneous otoacoustic emissions in the bobtail skink. J Neurophysiol 92, 2685-2693.

Marcotti, W., Corns, L.F., Desmonds, T., Kirkwood, N.K., Richardson, G.P., Kros, C.J., 2014. Transduction without tip links in cochlear hair cells is mediated by ion channels with permeation properties distinct from those of the mechano-electrical transducer channel. J Neurosci 34, 5505-5514.

Markowitz, A.L., Kalluri, R., 2020. Gradients in the biophysical properties of neonatal auditory neurons align with synaptic contact position and the intensity coding map of inner hair cells. Elife 9, e55378.

Martin, P., 2008. Active hair-bundle motility of the hair cells of vestibular and auditory organs. In: Manley, G.A., Popper, A.N., Fay, R.R. (Eds.), Active processes and otoacoustic emissions. Springer, New York, pp. 93-144.

Martin, P., Bozovic, D., Choe, Y., Hudspeth, A.J., 2003. Spontaneous oscillation by hair bundles of the bullfrog's sacculus. J Neurosci 23, 4533-4548.

Martin, P., Hudspeth, A.J., 1999. Active hair-bundle movements can amplify a hair cell's response to oscillatory mechanical stimuli. Proceedings of the National Academy of Sciences of the United States of America 96, 14306-14311.

Martin, P., Hudspeth, A.J., 2001. Compressive nonlinearity in the hair bundle's active response to mechanical stimulation. Proc Natl Acad Sci U S A 98, 14386-14391.

Meyer, A.C., Frank, T., Khimich, D., Hoch, G., Riedel, D., Chapochnikov, N.M., Yarin, Y.M., Harke, B., Hell, S.W., Egner, A., Moser, T., 2009. Tuning of synapse number, structure and function in the cochlea. Nat Neurosci 12, 444-453.

Moore, B.C., 1973. Frequency difference limens for short-duration tones. J Acoust Soc Am 54, 610-619.

Moore, B.C.J., 2004. An Introduction to the Psychology of Hearing, Fifth Edition ed. Elsevier Science & Technology Books, London.

Muller, M., von Hunerbein, K., Hoidis, S., Smolders, J.W., 2005. A physiological place-frequency map of the cochlea in the CBA/J mouse. Hear Res 202, 63-73.

Nadol, J.B., Jr., 1988. Comparative anatomy of the cochlea and auditory nerve in mammals. Hear Res 34, 253-266.

Nadrowski, B., Martin, P., Julicher, F., 2004. Active hair-bundle motility harnesses noise to operate near an optimum of mechanosensitivity. Proc Natl Acad Sci U S A 101, 12195-12200.

Naidu, R.C., Mountain, D.C., 1998. Measurements of the stiffness map challenge a basic tenet of cochlear theories. Hear Res 124, 124-131.

Narayan, S.S., Temchin, A.N., Recio, A., Ruggero, M.A., 1998. Frequency tuning of basilar membrane and auditory nerve fibers in the same cochleae. Science 282, 1882-1884.

Newsome, W.T., Britten, K.H., Movshon, J.A., 1989. Neuronal correlates of a perceptual decision. Nature 341, 52-54.

Ni, G., Elliott, S.J., Ayat, M., Teal, P.D., 2014. Modelling cochlear mechanics. Biomed Res Int 2014, 150637.

Niwa, M., Young, E.D., Glowatzki, E., Ricci, A.J., 2021. Functional subgroups of cochlear inner hair cell ribbon synapses differently modulate their EPSC properties in response to stimulation. J Neurophysiol 125, 2461-2479.

Nobili, R., Mammano, F., Ashmore, J., 1998. How well do we understand the cochlea? Trends Neurosci 21, 159-167.

Nuttall, A.L., Grosh, K., Zheng, J., de Boer, E., Zou, Y., Ren, T., 2004. Spontaneous basilar membrane oscillation and otoacoustic emission at 15 kHz in a guinea pig. J Assoc Res Otolaryngol 5, 337-348.

Nuttall, A.L., Ricci, A.J., Burwood, G., Harte, J.M., Stenfelt, S., Caye-Thomasen, P., Ren, T., Ramamoorthy, S., Zhang, Y., Wilson, T., Lunner, T., Moore, B.C.J., Fridberger, A., 2018. A mechanoelectrical mechanism for detection of sound envelopes in the hearing organ. Nat Commun 9, 4175.

O Maoileidigh, D., Hudspeth, A.J., 2013. Effects of cochlear loading on the motility of active outer hair cells. Proc Natl Acad Sci U S A 110, 5474-5479.

O Maoileidigh, D., Julicher, F., 2010. The interplay between active hair bundle motility and electromotility in the cochlea. J Acoust Soc Am 128, 1175-1190.

O Maoileidigh, D., Nicola, E.M., Hudspeth, A.J., 2012. The diverse effects of mechanical loading on active hair bundles. Proc Natl Acad Sci U S A 109, 1943-1948.

Ohlemiller, K.K., Siegel, J.H., 1994. Cochlear basal and apical differences reflected in the effects of cooling on responses of single auditory nerve fibers. Hear Res 80, 174-190.

Ohn, T.L., Rutherford, M.A., Jing, Z., Jung, S., Duque-Afonso, C.J., Hoch, G., Picher, M.M., Scharinger, A., Strenzke, N., Moser, T., 2016. Hair cells use active zones with different voltage dependence of Ca2+ influx to decompose sounds into complementary neural codes. Proc Natl Acad Sci U S A 113, E4716-4725.

Olson, E.S., Duifhuis, H., Steele, C.R., 2012. Von Bekesy and cochlear mechanics. Hear Res 293, 31-43.

Oxenham, A.J., 2012. Pitch perception. J Neurosci 32, 13335-13338.

Ozcete, O.D., Moser, T., 2021. A sensory cell diversifies its output by varying Ca(2+) influx-release coupling among active zones. EMBO J 40, e106010.

Palmer, A.R., Russell, I.J., 1986. Phase-locking in the cochlear nerve of the guinea-pig and its relation to the receptor potential of inner hair-cells. Hear Res 24, 1-15.

Panzeri, S., Brunel, N., Logothetis, N.K., Kayser, C., 2010. Sensory neural codes using multiplexed temporal scales. Trends Neurosci 33, 111-120.

Panzeri, S., Harvey, C.D., Piasini, E., Latham, P.E., Fellin, T., 2017. Cracking the Neural Code for Sensory Perception by Combining Statistics, Intervention, and Behavior. Neuron 93, 491-507.

Petitpre, C., Wu, H., Sharma, A., Tokarska, A., Fontanet, P., Wang, Y., Helmbacher, F., Yackle, K., Silberberg, G., Hadjab, S., Lallemend, F., 2018. Neuronal heterogeneity and stereotyped connectivity in the auditory afferent system. Nat Commun 9, 3691.

Pickles, J.O., 2003. An Introduction to the Physiology of Hearing, 2nd Edition ed, London.

Probst, R., 1990. Otoacoustic emissions: an overview. Adv Otorhinolaryngol 44, 1-91.

Pujol, R., Lenoir, M., Ladrech, S., Tribillac, F., Rebillard, G., 1992. Correlation Between the Length of Outer Hair Cells and the Frequency Coding of the Cochlea. In: Cazals, Y., Horner, K., Demany, L. (Eds.), Auditory Physiology and Perception. Pergamon, pp. 45-52.

Purcell, D.W., Ross, B., Picton, T.W., Pantev, C., 2007. Cortical responses to the 2f1-f2 combination tone measured indirectly using magnetoencephalography. J Acoust Soc Am 122, 992-1003.

Quiñones, P.M., Meenderink, S.W.F., Applegate, B.E., Oghalai, J.S., 2022. Unloading outer hair cell bundles in vivo does not yield evidence of spontaneous oscillations in the mouse cochlea. Hearing Research, 108473.

Rahman, M., Willmore, B.D.B., King, A.J., Harper, N.S., 2020. Simple transformations capture auditory input to cortex. Proc Natl Acad Sci U S A 117, 28442-28451.

Rattay, F., Potrusil, T., Wenger, C., Wise, A.K., Glueckert, R., Schrott-Fischer, A., 2013. Impact of morphometry, myelinization and synaptic current strength on spike conduction in human and cat spiral ganglion neurons. PLoS One 8, e79256.

Reichenbach, T., Hudspeth, A.J., 2010. A ratchet mechanism for amplification in low-frequency mammalian hearing. Proc Natl Acad Sci U S A 107, 4973-4978.

Reiter, E.R., Liberman, M.C., 1995. Efferent-mediated protection from acoustic overexposure: relation to slow effects of olivocochlear stimulation. J Neurophysiol 73, 506-514.

Ren, T., 2002. Longitudinal pattern of basilar membrane vibration in the sensitive cochlea. Proc Natl Acad Sci U S A 99, 17101-17106.

Ren, T., He, W., Kemp, D., 2016. Reticular lamina and basilar membrane vibrations in living mouse cochleae. Proc Natl Acad Sci U S A 113, 9910-9915.

Ren, T., He, W., Scott, M., Nuttall, A.L., 2006. Group delay of acoustic emissions in the ear. J Neurophysiol 96, 2785-2791.

Reyes, A.D., 2021. Mathematical framework for place coding in the auditory system. PLoS Comput Biol 17, e1009251.

Rhode, W.S., 1971. Observations of the vibration of the basilar membrane in squirrel monkeys using the Mossbauer technique. J Acoust Soc Am 49, Suppl 2:1218+.

Rhode, W.S., 2007. Distortion product otoacoustic emissions and basilar membrane vibration in the 6-9 kHz region of sensitive chinchilla cochleae. J Acoust Soc Am 122, 2725-2737.

Rhode, W.S., Robles, L., 1974. Evidence from Mossbauer experiments for nonlinear vibration in the cochlea. J Acoust Soc Am 55, 588-596.

Ricci, A.J., Crawford, A.C., Fettiplace, R., 2003. Tonotopic variation in the conductance of the hair cell mechanotransducer channel. Neuron 40, 983-990.

Ricci, A.J., Fettiplace, R., 1997. The effects of calcium buffering and cyclic AMP on mechano-electrical transduction in turtle auditory hair cells. J. Physiol. 501, 111-124.

Ricci, A.J., Gray-Keller, M., Fettiplace, R., 2000. Tonotopic variations of calcium signalling in turtle auditory hair cells. J. Physiol. 524 Pt 2, 423-436.

Ricci, A.J., Kennedy, H.J., Crawford, A.C., Fettiplace, R., 2005. The transduction channel filter in auditory hair cells. J Neurosci 25, 7831-7839.

Richter, C.P., Edge, R., He, D.Z., Dallos, P., 2000. Development of the gerbil inner ear observed in the hemicochlea. J Assoc Res Otolaryngol 1, 195-210.

Richter, C.P., Emadi, G., Getnick, G., Quesnel, A., Dallos, P., 2007. Tectorial membrane stiffness gradients. Biophys J 93, 2265-2276.

Riehle, A., Grun, S., Diesmann, M., Aertsen, A., 1997. Spike synchronization and rate modulation differentially involved in motor cortical function. Science 278, 1950-1953.

Robles, L., Ruggero, M.A., 2001. Mechanics of the mammalian cochlea. Physiol Rev 81, 1305-1352.

Robles, L., Ruggero, M.A., Rich, N.C., 1986. Basilar membrane mechanics at the base of the chinchilla cochlea. I. Input-output functions, tuning curves, and response phases. J Acoust Soc Am 80, 1364-1374.

Robles, L., Ruggero, M.A., Rich, N.C., 1991. Two-tone distortion in the basilar membrane of the cochlea. Nature 349, 413-414.

Robles, L., Ruggero, M.A., Rich, N.C., 1997. Two-tone distortion on the basilar membrane of the chinchilla cochlea. J Neurophysiol 77, 2385-2399.

Romero, G.E., Trussell, L.O., 2021. Distinct forms of synaptic plasticity during ascending vs descending control of medial olivocochlear efferent neurons. Elife 10, e66396.

Rose, J.E., Brugge, J.F., Anderson, D.J., Hind, J.E., 1967. Phase-locked response to low-frequency tones in single auditory nerve fibers of the squirrel monkey. J Neurophysiol 30, 769-793.

Roth, B., Bruns, V., 1992. Postnatal development of the rat organ of Corti. II. Hair cell receptors and their supporting elements. Anat Embryol (Berl) 185, 571-581.

Ruggero, M.A., Rich, N.C., 1991. Application of a commercially-manufactured Doppler-shift laser velocimeter to the measurement of basilar-membrane vibration. Hear Res 51, 215-230.

Ruggero, M.A., Rich, N.C., Recio, A., Narayan, S.S., Robles, L., 1997. Basilar-membrane responses to tones at the base of the chinchilla cochlea. J Acoust Soc Am 101, 2151-2163.

Ruggero, M.A., Robles, L., Rich, N.C., 1992. Two-tone suppression in the basilar membrane of the cochlea: mechanical basis of auditory-nerve rate suppression. J Neurophysiol 68, 1087-1099.

Ruggero, M.A., Temchin, A.N., 2007. Similarity of traveling-wave delays in the hearing organs of humans and other tetrapods. J Assoc Res Otolaryngol 8, 153-166.

Rusch, A., Thurm, U., 1990. Spontaneous and electrically induced movements of ampullary kinocilia and stereovilli. Hear Res 48, 247-263.

Russell, I.J., Drexl, M., Foeller, E., Vater, M., Kossl, M., 2003. Synchronization of a nonlinear oscillator: processing the cf component of the echo-response signal in the cochlea of the mustached bat. J Neurosci 23, 9508-9518.

Russell, I.J., Kossl, M., Richardson, G.P., 1992. Nonlinear mechanical responses of mouse cochlear hair bundles. Proc Biol Sci 250, 217-227.

Russell, I.J., Murugasu, E., 1997. Medial efferent inhibition suppresses basilar membrane responses to near characteristic frequency tones of moderate to high intensities. J Acoust Soc Am 102, 1734-1738.

Russell, I.J., Nilsen, K.E., 1997. The location of the cochlear amplifier: spatial representation of a single tone on the guinea pig basilar membrane. Proc Natl Acad Sci U S A 94, 2660-2664.

Russell, I.J., Richardson, G.P., Kossl, M., 1989. The responses of cochlear hair cells to tonic displacements of the sensory hair bundle. Hear Res 43, 55-69.

Russell, I.J., Sellick, P.M., 1983. Low-frequency characteristics of intracellularly recorded receptor potentials in guinea-pig cochlear hair cells. J Physiol 338, 179-206.

Salvi, J.D., D, O.M., Fabella, B.A., Tobin, M., Hudspeth, A.J., 2015. Control of a hair bundle's mechanosensory function by its mechanical load. Proc Natl Acad Sci U S A 112, E1000-1009.

Salvi, J.D., D, O.M., Hudspeth, A.J., 2016. Identification of Bifurcations from Observations of Noisy Biological Oscillators. Biophys J 111, 798-812.

Santos-Sacchi, J., 1992. On the frequency limit and phase of outer hair cell motility: effects of the membrane filter. J Neurosci 12, 1906-1916.

Santos-Sacchi, J., Dilger, J.P., 1988. Whole cell currents and mechanical responses of isolated outer hair cells. Hear Res 35, 143-150.

Santos-Sacchi, J., Kakehata, S., Kikuchi, T., Katori, Y., Takasaka, T., 1998. Density of motility-related charge in the outer hair cell of the guinea pig is inversely related to best frequency. Neuroscience Letters 256, 155-158.

Schnee, M.E., Lawton, D.M., Furness, D.N., Benke, T.A., Ricci, A.J., 2005. Auditory hair cell-afferent fiber synapses are specialized to operate at their best frequencies. Neuron 47, 243-254.

Schnupp, J., Nelken, I., King, A., 2011. Auditory neuroscience : making sense of sound. MIT Press, Cambridge, Mass.

Schooneveldt, G.P., Moore, B.C.J., 1989. Comodulation Masking Release (Cmr) as a Function of Masker Bandwidth, Modulator Bandwidth, and Signal Duration. Journal of the Acoustical Society of America 85, 273-281.

Sellick, P.M., Patuzzi, R., Johnstone, B.M., 1982. Measurement of Basilar-Membrane Motion in the Guinea-Pig Using the Mossbauer Technique. Journal of the Acoustical Society of America 72, 131-141.

Shaw, E.A.G., 1974. The External Ear. In: Neff, W.D.K.a.W.D. (Ed.), Springer, Berlin, pp. 455-490.

Shera, C.A., 2003. Mammalian spontaneous otoacoustic emissions are amplitude-stabilized cochlear standing waves. J Acoust Soc Am 114, 244-262.

Shera, C.A., 2007. Laser amplification with a twist: traveling-wave propagation and gain functions from throughout the cochlea. J Acoust Soc Am 122, 2738-2758.

Shera, C.A., Guinan, J.J., Jr., Oxenham, A.J., 2002. Revised estimates of human cochlear tuning from otoacoustic and behavioral measurements. Proc Natl Acad Sci U S A 99, 3318-3323.

Sherrill, H.E., Jean, P., Driver, E.C., Sanders, T.R., Fitzgerald, T.S., Moser, T., Kelley, M.W., 2019. Pou4f1 Defines a Subgroup of Type I Spiral Ganglion Neurons and Is Necessary for Normal Inner Hair Cell Presynaptic Ca(2+) Signaling. J Neurosci 39, 5284-5298.

Shotwell, S.L., Jacobs, R., Hudspeth, A.J., 1981. Directional sensitivity of individual vertebrate hair cells to controlled deflection of their hair bundles. Ann N Y Acad Sci 374, 1-10.

Shrestha, B.R., Chia, C., Wu, L., Kujawa, S.G., Liberman, M.C., Goodrich, L.V., 2018. Sensory Neuron Diversity in the Inner Ear Is Shaped by Activity. Cell 174, 1229-1246 e1217.

Siegel, J.H., 1992. Spontaneous synaptic potentials from afferent terminals in the guinea pig cochlea. Hear Res 59, 85-92.

Sivian, L.J., White, S.D., 1933. On minimum audible sound fields. J. Acoust. Soc. Am. 4, 288-321.

Spoendlin, H., 1969. Innervation patterns in the organ of corti of the cat. Acta Otolaryngol 67, 239-254.

Spoendlin, H., 1972. Innervation densities of the cochlea. Acta Otolaryngol 73, 235-248.

Stevens, S.S., 1957. On the psychophysical law. Psychol Rev 64, 153-181.

Sullivan, W.E., Konishi, M., 1984. Segregation of stimulus phase and intensity coding in the cochlear nucleus of the barn owl. J Neurosci 4, 1787-1799.

Sun, S., Babola, T., Pregernig, G., So, K.S., Nguyen, M., Su, S.M., Palermo, A.T., Bergles, D.E., Burns, J.C., Muller, U., 2018. Hair Cell Mechanotransduction Regulates Spontaneous Activity and Spiral Ganglion Subtype Specification in the Auditory System. Cell 174, 1247-1263 e1215.

Swabey, M., Chambers, P., Lutman, M.L., White, N.M., Chad, J.E., Brown, A.D., Beeby, S.P., 2009. The biometric potential of transient otoacoustic emissions. International Journal of Biometrics 1, 349-364.

Taberner, A.M., Liberman, M.C., 2005. Response properties of single auditory nerve fibers in the mouse. J Neurophysiol 93, 557-569.

Tan, X., Wang, X., Yang, W., Xiao, Z., 2008. First spike latency and spike count as functions of tone amplitude and frequency in the inferior colliculus of mice. Hear Res 235, 90-104.

Tartini, G., 1754. Trattato di musica secondo la vera scienza dell'armonia. G. Manfré, Padova.

Tasaki, I., 1954. Nerve impulses in individual auditory nerve fibers of guinea pig. J Neurophysiol 17, 97-122.

Tilney, L.G., Saunders, J.C., 1983. Actin filaments, stereocilia, and hair cells of the bird cochlea. I. Length, number, width, and distribution of stereocilia of each hair cell are related to the position of the hair cell on the cochlea. J Cell Biol 96, 807-821.

Tinevez, J.Y., Julicher, F., Martin, P., 2007. Unifying the various incarnations of active hair-bundle motility by the vertebrate hair cell. Biophys J 93, 4053-4067.

Tobin, M., Chaiyasitdhi, A., Michel, V., Michalski, N., Martin, P., 2019. Stiffness and tension gradients of the hair cell's tip-link complex in the mammalian cochlea. Elife 8, e43473.

Turner, R.G., Muraski, A.A., Nielsen, D.W., 1981. Cilium length: influence on neural tonotopic organization. Science 213, 1519-1521.

Ulehlova, L., Voldrich, L., Janisch, R., 1987. Correlative study of sensory cell density and cochlear length in humans. Hear Res 28, 149-151.

Vassilakis, P.N., Meenderink, S.W., Narins, P.M., 2004. Distortion product otoacoustic emissions provide clues hearing mechanisms in the frog ear. J Acoust Soc Am 116, 3713-3726.

Vavakou, A., Cooper, N.P., van der Heijden, M., 2019. The frequency limit of outer hair cell motility measured in vivo. Elife 8, e47667.

Verpy, E., Leibovici, M., Michalski, N., Goodyear, R.J., Houdon, C., Weil, D., Richardson, G.P., Petit, C., 2011. Stereocilin connects outer hair cell stereocilia to one another and to the tectorial membrane. J Comp Neurol 519, 194-210.

Verpy, E., Weil, D., Leibovici, M., Goodyear, R.J., Hamard, G., Houdon, C., Lefevre, G.M., Hardelin, J.P., Richardson, G.P., Avan, P., Petit, C., 2008. Stereocilin-deficient mice reveal the origin of cochlear waveform distortions. Nature 456, 255-258.

Verschooten, E., Shamma, S., Oxenham, A.J., Moore, B.C.J., Joris, P.X., Heinz, M.G., Plack, C.J., 2019. The upper frequency limit for the use of phase locking to code temporal fine structure in humans: A compilation of viewpoints. Hear Res 377, 109-121.

Vogel, A., Ronacher, B., 2007. Neural correlations increase between consecutive processing levels in the auditory system of locusts. J Neurophysiol 97, 3376-3385.

Volkov, I.O., Galazjuk, A.V., 1991. Formation of spike response to sound tones in cat auditory cortex neurons: interaction of excitatory and inhibitory effects. Neuroscience 43, 307-321.

von Békésy, G.V., 1956. Current status of theories of hearing. Science 123, 779-783.

von Békésy, G.V., 1960. Experiments in hearing, Translated and edited by E. G. Wever ed. McGraw-Hill, London.

Warr, W.B., Guinan, J.J., Jr., 1979. Efferent innervation of the organ of corti: two separate systems. Brain Res 173, 152-155.

Warren, R.L., Ramamoorthy, S., Ciganovic, N., Zhang, Y., Wilson, T.M., Petrie, T., Wang, R.K., Jacques, S.L., Reichenbach, T., Nuttall, A.L., Fridberger, A., 2016. Minimal basilar membrane motion in low-frequency hearing. Proc Natl Acad Sci U S A 113, E4304-4310.

Weber, E.H., 1851. Die Lehre vom Tastsinn und Gemeingefühl, auf Versuche gegründet. Vieweg, Braunschweig, Germany.

Weiss, T.F., 1982. Bidirectional transduction in vertebrate hair cells: a mechanism for coupling mechanical and electrical processes. Hear Res 7, 353-360.

Weisz, C., Glowatzki, E., Fuchs, P., 2009. The postsynaptic function of type II cochlear afferents. Nature 461, 1126-1129.

Weisz, C.J.C., Williams, S.G., Eckard, C.S., Divito, C.B., Ferreira, D.W., Fantetti, K.N., Dettwyler, S.A., Cai, H.M., Rubio, M.E., Kandler, K., Seal, R.P., 2021. Outer Hair Cell Glutamate Signaling through Type II Spiral Ganglion Afferents Activates Neurons in the Cochlear Nucleus in Response to Nondamaging Sounds. J Neurosci 41, 2930-2943.

Wen, B., Wang, G.I., Dean, I., Delgutte, B., 2009. Dynamic range adaptation to sound level statistics in the auditory nerve. J Neurosci 29, 13797-13808.

Wever, E.G., Bray, C.W., 1930. Present possibilities for auditory theory. Psychological Review 37, 365-380.

Wiederhold, M.L., Kiang, N.Y., 1970. Effects of electric stimulation of the crossed olivocochlear bundle on single auditory-nerve fibers in the cat. J Acoust Soc Am 48, 950-965.

Wilent, W.B., Contreras, D., 2005. Dynamics of excitation and inhibition underlying stimulus selectivity in rat somatosensory cortex. Nat Neurosci 8, 1364-1370.

Wilson, J.P., 1980. Evidence for a cochlear origin for acoustic re-emissions, threshold fine-structure and tonal tinnitus. Hear Res 2, 233-252.

Winslow, R.L., Sachs, M.B., 1987. Effect of electrical stimulation of the crossed olivocochlear bundle on auditory nerve response to tones in noise. J Neurophysiol 57, 1002-1021.

Wong, A.B., Jing, Z., Rutherford, M.A., Frank, T., Strenzke, N., Moser, T., 2013. Concurrent maturation of inner hair cell synaptic Ca2+ influx and auditory nerve spontaneous activity around hearing onset in mice. J Neurosci 33, 10661-10666.

Wright, A., 1984. Dimensions of the cochlear stereocilia in man and the guinea pig. Hear Res 13, 89-98.

Wu, Y.C., Ricci, A.J., Fettiplace, R., 1999. Two components of transducer adaptation in auditory hair cells. J Neurophysiol 82, 2171-2181.

Zandvakili, A., Kohn, A., 2015. Coordinated Neuronal Activity Enhances Corticocortical Communication. Neuron 87, 827-839.

Zhao, Y., Yamoah, E.N., Gillespie, P.G., 1996. Regeneration of broken tip links and restoration of mechanical transduction in hair cells. Proc Natl Acad Sci U S A 93, 15469-15474.

Zheng, J., Shen, W., He, D.Z., Long, K.B., Madison, L.D., Dallos, P., 2000. Prestin is the motor protein of cochlear outer hair cells. Nature 405, 149-155.

Zorowka, P.G., 1993. Otoacoustic emissions: a new method to diagnose hearing impairment in children. Eur J Pediatr 152, 626-634.

Zurek, P.M., Clark, W.W., 1981. Narrow-Band Acoustic-Signals Emitted by Chinchilla Ears after Noise Exposure. Journal of the Acoustical Society of America 70, 446-450.

Zweig, G., 1991. Finding the impedance of the organ of Corti. J Acoust Soc Am 89, 1229-1254.

Zwicker, E., 1961. Subdivision of Audible Frequency Range into Critical Bands (Frequenzgruppen). Journal of the Acoustical Society of America 33, 248-&.

Zwislocki, J.J., Kletsky, E.J., 1979. Tectorial membrane: a possible effect on frequency analysis in the cochlea. Science 204, 639-641.